BTA/TGP/11-07

Title

Reservoir Grain analysis and correlation of GR-log to cuttings

for the Ammerlaan geothermal well PNA GT01

Date 23/06/11

Student name H.E.J. van Oeveren

Department of Geotechnology

Delft University of Technology

Title	:	Reservoir Grain analysis and correlation of GR-log to cuttings for the Ammerlaan geothermal well PNA GT01
Author(s)	:	H.E.J. van Oeveren
Date	:	June 2011
Professor(s)	:	Dr. K.H.A.A. Wolf
Supervisor(s)	:	Dr. Ir. E.S.J. Rudolph
TA Report number	:	BTA/TGP/11-07
Postal Address	:	Section for Applied Geophysics and Petrophysics Department of Applied Earth Sciences Delft University of Technology P.O. Box 5028 The Netherlands
Telephone	:	(31) 15 2781328 (secretary)
Telefax	:	(31) 15 2781189

Abstract

The Delft Geothermal Project is an ongoing study of the subsurface of the Delft and Pijnacker area with the aim to assist in geothermal projects. The industry has an interest in warm subsurface water for the heating of buildings. In scope of the project this study examines the cuttings collected from the production well of a geothermal doublet for a greenhouse farmer in Pijnacker. Geothermal power produced by this farmer will be used to warm up a greenhouse, a swimming pool and a school.

The geothermal doublet produces water from the Delft Sandstone member. The Delft Sandstone member is a fluvial deposit from the Schieland group. It was deposited in the West Netherlands Basin during the Late Jurassic to Early Cretaceous.

The production well is called the PNA GT01. In the well path of this production well the top of the Delft Sandstone member is found at a true vertical depth of 2138 meters. The member has a thickness of 64 meters. The aim of this project is to give a description of the Delft Sandstone member based on the cuttings of the PNA GT01 well. When the production well was drilled the rock fragments were transported from the drill bit to the surface in suspension in a brine drilling mud. These cutting samples were collected at the surface. The cuttings were sieved and dried as a preparation for the examination.

The examination of the content was performed using a stereo microscope and a comparator card. The results show cuttings consisting of claystone, siltstone, sand and coal seams.
The cuttings were examined on hydrocarbon content using ultra violet light and a camera. This examination shows hydrocarbon occurrence in the entire Delft Sandstone member.
The gamma ray, the shale content, the grain size estimation, and the hydrocarbon content and cutting content are presented graphically.
The silt fraction was flushed when the dried cuttings were prepared; this fraction was not examined in the study. As a consequence the Gamma ray predicts a higher shale contents than is expected from the cutting analysis.

The results of this report can be used as a database in models of the Delft Sandstone member.

Table of Contents

Abstract 2

Table of Contents 3

The Assignment – BSC contract 4

Chapter 1 - Introduction 5

Chapter 2 - Geology of the reservoir 7

Chapter 3 - Stratigraphy of the West Netherlands Basin in view of the reservoir properties 8

The reservoir 11

Chapter 4 - Data and Methods 11

Gathering of data while drilling 11

Processing and preparation of the cutting samples 13

Cutting analysis 14

Hydrocarbon content 14

Gamma ray log interpretation and correlation to the cutting samples 16

Flow chart of cutting analysis from collection to implementation 16

Chapter 5 - Cutting content and grain size estimation with XRF and Microscope 17

Chapter 6 - Sample description of GT01 Delft Sandstone member and correlation to gamma ray using 3 characteristic intervals 19

Interval 2738 – 2748 19

Interval 2770-2778 20

Interval 2748- 2757 21

Chapter 7 - Hydrocarbon content 23

Chapter 8 - Results of correlations 24

The gamma ray log, cutting content estimation, grain size and the shale content of the PNA GT01 well 25

Chapter 9 – Discussion and Conclusions 27

Recommendations 28

Acknowledgements 28

References 29

Supplementary data 30

Interval Rodenrijs Claystone-2738 30

Interval 2738 – 2748 31

Interval 2748- 2757 33

Interval 2757-2763 35

Interval 2763-2770 36

Interval 2770-2778 37
Interval 2778-2788 38
Interval 2788-2796 40
Interval 2796-2811 41
Interval 2811-2814 41
Interval 2814-2818 43
Interval 2818-2825 44
Interval 2825- Alblasserdam 45
Hydrocarbon content in wet cutting samples 46
Hydrocarbon fluorescence in dried cutting samples.......... 48
Content of cutting samples – fine fraction 49
Content of cutting samples – course fraction 50
Data from the XRF analysis 51

The Assignment – BSC contract

Correlation of GR-log to cuttings for Ammerlaan Wells.

When the two wells were drilled a gamma-ray tool was used to measure the level of gamma-radiation that emanates from the rock. The natural radiation can be used to predict the shale content of the rock. A correlation of the gamma-ray log and the cuttings from a well can be used for a description of the rock.

CT-scans of selected cuttings of Ammerlaan wells to determine porosity and permeability
A micro-CT-scanner makes it possible to recognise grain features and pore sizes up to 10 micrometre. Relevant are the quality of CT-images and pixel resolution. In this project several types of grains have to be cleaned (removal of heavy drilling fluid) and scanned with XRD, XRF and the CT scan.
The grains will have to be examined using a SEM. This is to examine the permeability and porosity characteristic of the reservoir.

Type of activities for the students (theoretical work, practical work, etc.).

1. Simple cutting analysis
2. correlation of cuttings to gamma-ray well data
3. Analysis and reconstruction of the reservoir grains using SEM, XRD,XRF and CT-scan.
4. Analysis of reservoir fluid

Points 1 and 2 have been executed:
All the available cuttings from the reservoir where examined using a stereomicroscope and a comparator card.
An overview of the content of the cuttings is presented.
Image of the cuttings are presented.

A grain size estimation of the cuttings is presented.
The cuttings are correlated to the gamma ray using intervals.

Point 4 and a part of point 3 have been executed by another party:
The analysis of the reservoir fluid was performed by Laura van Leeuwen and Joelle Langeveld.
The XRD-XRF analysis was performed by Laura van Leeuwen and Joelle van Langeveld.

Point 3 was partly not carried out:
No CT-scan was performed.
No reconstruction of the reservoir grains was made.

The contract was a combination of two proposed projects. Early on in the project the second part of the project was cancelled by Remco Groeneberg due to the time constraint of six weeks. The focus was on the cutting analysis and the correlation of cuttings to gamma-ray well data.

Chapter 1 - Introduction

The Netherlands have a short history in Deep Geothermal Energy. In 2006 the first deep geothermal project in the Netherlands was completed, Mijnwaterproject in Heerlen. The source of energy is the heat generated by depletion of radioactive elements in the core of the earth. This heat generated inside the earth gradually increases the temperature of the subsurface with increasing depth. This is called the geothermal gradient. The groundwater in the subsurface has the same temperature as the rock it is in. In deep geothermal projects this heated water is produced.

The Delft Geothermal Project (Delft Aardwarmte Project-DAP) was founded in 2008 by students of the TU Delft. Its goal is to assist in and to learn from geothermal projects in the Delft and Pijnacker area. In August of 2009 the DAP received the license to produce geothermal power in this area. The first industrial project completed with the help of the DAP is the Ammerlaan geothermal doublet in Pijnacker in 2010.

Ammerlaan Grond en Hydrocultuur is a greenhouse farmer in the village of Pijnacker. In this 40.000 m^2 large greenhouse the farmer nurtures tropical plants. Heating this greenhouse consumes a lot of energy. Natural gas was used to warm up water; the heated water was then pumped through the greenhouse to sustain a tropical climate. Warm water produced from geothermal wells can deliver more than enough energy to heat up the greenhouse. In 2010 the farmer decided to use geothermal power to heat the greenhouse. The surplus in warmth will be used to heat a nearby school and a swimming pool.

Ammerlaan uses the Delft Sandstone as a reservoir. The Delft Sandstone is a fluvial deposit from the Late Jurassic to Early Cretaceous. It consists of sand and clay deposits with coal seams in between. The reservoir for the Ammerlaan doublet is located at a true vertical depth of 2229,5 meters. In the Delft area the earth has a geothermal gradient of 3.1 degrees for every 100 meters (Smits, 2008). In the reservoir the water has a temperature of approximately 78°C (Gilding, 2010)

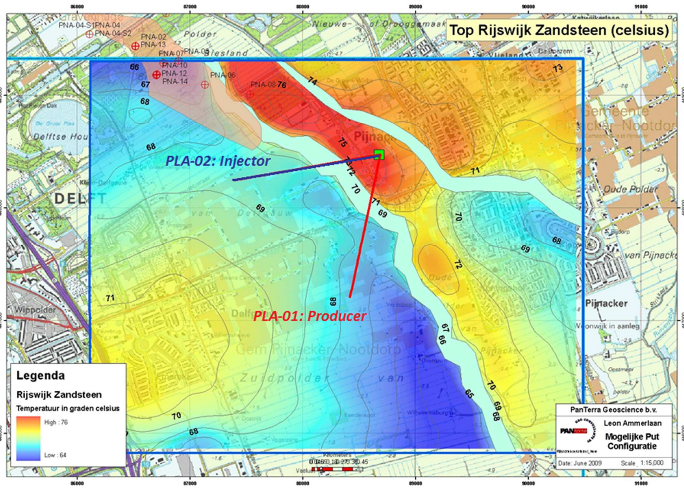

Figure 1 The doublet of geothermal wells as they were drilled in Pijnacker, from the Drilling program of PNA GT-01 (Smeulders, 2010) picture of Panterra

The two wells were drilled between May and October of 2010. One well, the PNA GT02, was meant to produce water. The other well, PNA GT01, was meant to inject cold water. This set-up changed later on in the project. When the wells were drilled the natural radiation of the rock was measured using a gamma ray tool. This data is presented in a gamma ray log. Also drilling samples were collected from the drilling mud. The drilling mud transports cuttings from the rock to the surface. At the surface these cuttings were collected.

When the farmer started production in November 2010 they produced carbon dioxide and water. The farmer experienced difficulties in injecting the cold water back into the reservoir. To improve performance of the doublet the production and injection wells were swapped. The former injection well PNA-GT01 became the production well and vice verse. Together with the water produced from the new production well the farmer produced methane and after a while heavier hydrocarbons.

The purpose of this report is to present the content of the Delft Sandstone reservoir at the Pijnacker location. The cuttings show the composition of the rock. The report also shows the occurrence of hydrocarbons over the entire depth of the reservoir. The result of the cutting analysis is correlated to the gamma ray log.
This report can be used to optimise existing reservoir models or to create new models for future projects in the Delft sandstone.

Chapter 2 - Geology of the reservoir

Within the framework of the use of the Delft Sandstone for this geothermal project the regional geology has been reevaluated. Previous studies are known (Gilding, 2010), (Smits, 2008), (Drost & Korenromp, 2010) and (Wiggers, 2009). The literature studies are used to get an understanding of the expected lithology in the Delft Sandstone member and the members surrounding it.

The West Netherlands Basin.

The reservoir was deposited in the West Netherlands Basin. The basin is located in the southwest of the Netherlands. At the south the Basin is bounded by the London-Brabant Massif. To the north the Basin is bounded by the Zandvoort Ridge and the Ijmuiden High. (Bogaeart & Kouwe, 1993).

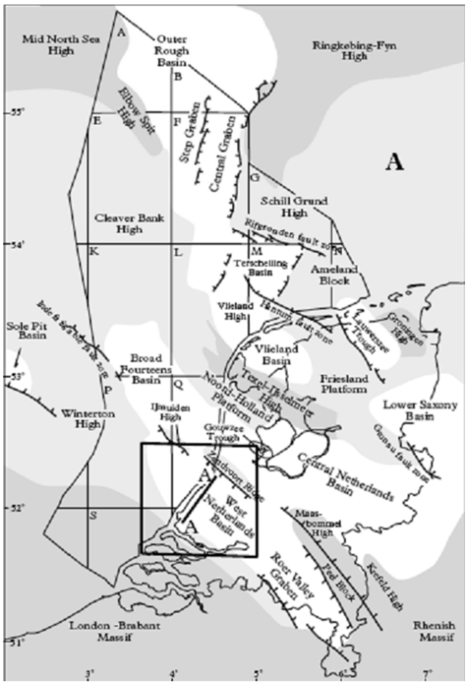

Figuur 2 The West Netherlands Basin NJG van Balen, modified after van Adrichem Bogaeart & Kouwe, 1993

The history of the West Netherlands basin will be described in four stages: the Late Carboniferous-the Early Permian stage, the Late Permian-The Middle Jurassic pre-rift stage, the Late Jurassic- the Early Cretaceous syn-rift stage and the Late Cretaceous- Quaternary post-rift and inversion stage. (Van Balen, et al., 2000)

Late Carboniferous –Early Permian

From the Late Carboniferous till the Early Permian stage the WNB was part of the Vascian Basin. In this stage the Variscan orogeny (Westphalian-Early Permian) caused major faulting, uplift and erosion in the basin. In the Northern part of the basin 500 meters of the Zandvoort Ridge sediments where eroded. Due to this uplifting the erosion was much less in the south. (Van Balen, et al., 2000)

Late Permian-Middle Jurassic

In the Late Permian-Middle Jurassic the basin was uplifted. This uplift was followed by regional thermal subsidence in the Early Triassic. The Lower and Middle Jurassic sediments consist of mainly marine shales including the Lower Jurassic kerogen-rich Posidonia Shale, the main source of oil in the West Netherlands Basin. (Rondeel, Batjes, & Nieuweenhuijs, 1996). Under a small northward dip the sedimentary succession consists of mainly fluvial and Aeolian sandstones of the upper Rotliegend Group, covered by claystones, siltstones and carbonates of the Zechstein Group. In the Middle-Late Triassic the WNB formed a half-graben, bounded in the North by a major fault zone (Van Balen, et al., 2000).

Late Jurassic-Early Cretaceous

The Late Jurassic to Early Cretaceous is a period of strong rifting. The rifting caused the breaking-up of the basin in various subunits with large variations in thicknesses in the Late Jurassic basin infill. Locally the sand and clay infill was more than 2500 meters thick; this infill belongs to the continental Schieland group. The subject of this report, the Delft Sandstone member, belongs to this group. The uplift of adjacent platforms resulted in a widely recognized unconformity.
After this uplift a large open marine basin formed in which the Rijnland group was deposited. The Rijnland Group consists of mainly fine-grained clastic sediment with coastal sandstones of up to 1400

meters thick. (De Jager, Doyle, Grantham, & Mabillard, 1996)
This stage was accompanied by repeated igneous activity in the Southeastern part of the basin. This indicates deep crustal fracturing.
In the Late Cretaceous the rifting stopped, however the subsidence continued. (Wong, 2007)

Late Cretaceous-Quaternary

The Late Cretaceous to the Quaternary is the post-rift and inversion stage. The rifting ceased in the Late Cretaceous and the Alpine orogeny caused the inversion in the WNB. In turn this led to the oil bearing structures in the basin. (Van Balen, et al., 2000)
During the Maastrichtian Danian when the inversion temporarily ceased the whole basin was covered with sediments.
In the Paleogene the basin was uplifted and hardly any sedimentation took place. The uplift was followed by a subsidence in the Neogene.
During the syn-rift stage the WNB was filled with sediment from fluvial systems from the southeast, the rivers followed the Northeast Southwest trend of the basin. In the Northeast the sea found its way into the basin. In the basin an there was interfingering of fluvial and marine sediment. (Wong, 2007)

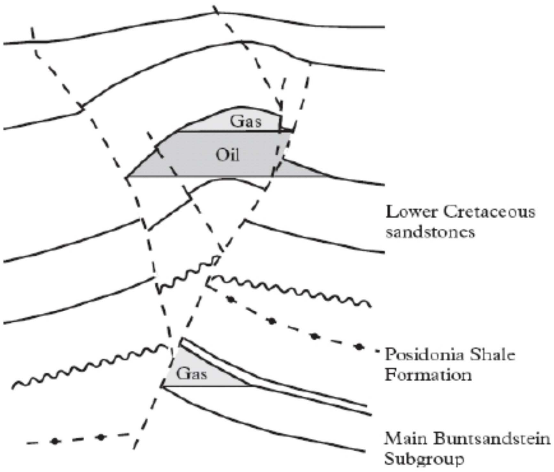

Figure 3 Trap situation as was created during the Early Cretaceous (van Balen, 2000)

Chapter 3 - Stratigraphy of the West Netherlands Basin in view of the reservoir properties

The deposits from the West Netherlands basin, as was previously described, can be subdivided in groups, subgroups, formations and members. The lithology of the region is described below in order to give a description of the lithology that is expected in and near the reservoir.

In the west Netherlands basin three groups of sediments were deposited during the Mesozoic era. The Chalk group is the group deposited during the upper Cretaceous. Below this group the Rijnland group was deposited during the Lower Cretaceous and the Schieland Group was formed during the Upper

Jurassic to the Lower Cretaceous. Our reservoir is a member of the Schieland group.

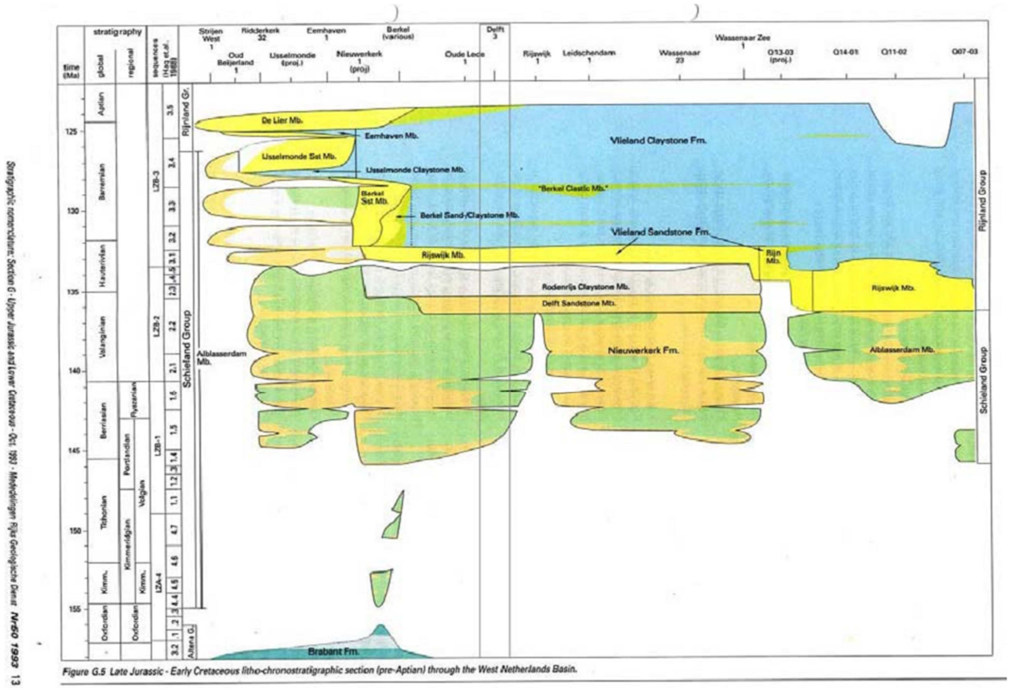

Figure 1 Litho-Chronostratigraphic section through the West Netherlands Basin, the stacking and stratigraphy of the different Members is shown (After Van Adrichem Boogaert & Kouwe, 1993)

<u>The Schieland group (SL)</u>

Geothermal projects of the Delft Aardwarmte Project have their main focus on the Schieland group. The Schieland group consists of all the deposits from the Central Graben subgroup (SLC) and the Delftland Subgroup (SLD). The deposits from the Schieland group consist of coaly to clayey sandstones, grey and colourful claystones and coal seams. (Bogaeart & Kouwe, 1993)

<u>The Delftland subgroup (SLD)</u>

The Delftland subgroup includes all the formations deposited in the Vlieland Basin, the Central Netherlands basin, the Broad Fourteens Basin, the West Netherlands Basin and the Roer Valley Graben.

<u>The Nieuwekerk Formation (SLDN)</u>

The Nieuwekerk Formation deposits occur in the West Netherlands Basin and the Roer Valley Graben. The Nieuwekerk Formation contains a sequence of typically dark or light grey, red or colourful claystones, fine to medium grained sandstones and course grained thick bedded sandstones. The grey claystones contain rare coal seams (Bogaeart & Kouwe, 1993)

<u>The Alblasserdam Member (SLDNA)</u>

The Alblasserdam Member is the oldest member of the Nieuwekerk formation. The member was deposited during the Ryazanian to the Valanginian age. The Alblasserdam Member consists predominantly of fluvial plain deposits varying between 100 and 1300 meters in thickness. This height variation is due to syn-rift deposition and rapid pinch-out in a southwest direction towards the London Brabant Massif.

In the Channels of the Alblasserdam Member sand was concentrated and the floodplains formed swamp and soil deposits. The dominant transport direction is from the southeast to the northwest (Bogaeart & Kouwe, 1993).

Sediments in the Alblasserdam Member are beige or light grey, firm and partly sandy siltstones with abundant darkish brown to black-brown laminated claystone. Occasionally colourless pale medium to fine grained sandstone is found in the Alblasserdam Member. The grey claystones consist of coal and lignite seams (Drost & Korenromp, 2010). Within the member lignite matter, siderite spherules and concretions can be found. In the Alblasserdam member gastropods can be found. Gastropods are turbinate shells not found in the cutting samples of the Delft Sandstone members.

The Delft Sandstone Member (SLDND)

The Delft Sandstone member is of Valanginian age and is distributed in the western and central parts of the West Netherlands Basin. The member varies in thickness between almost zero to 130 meters. (Smits, 2008). Syn-rift deposition of sediments caused the variation in thickness.

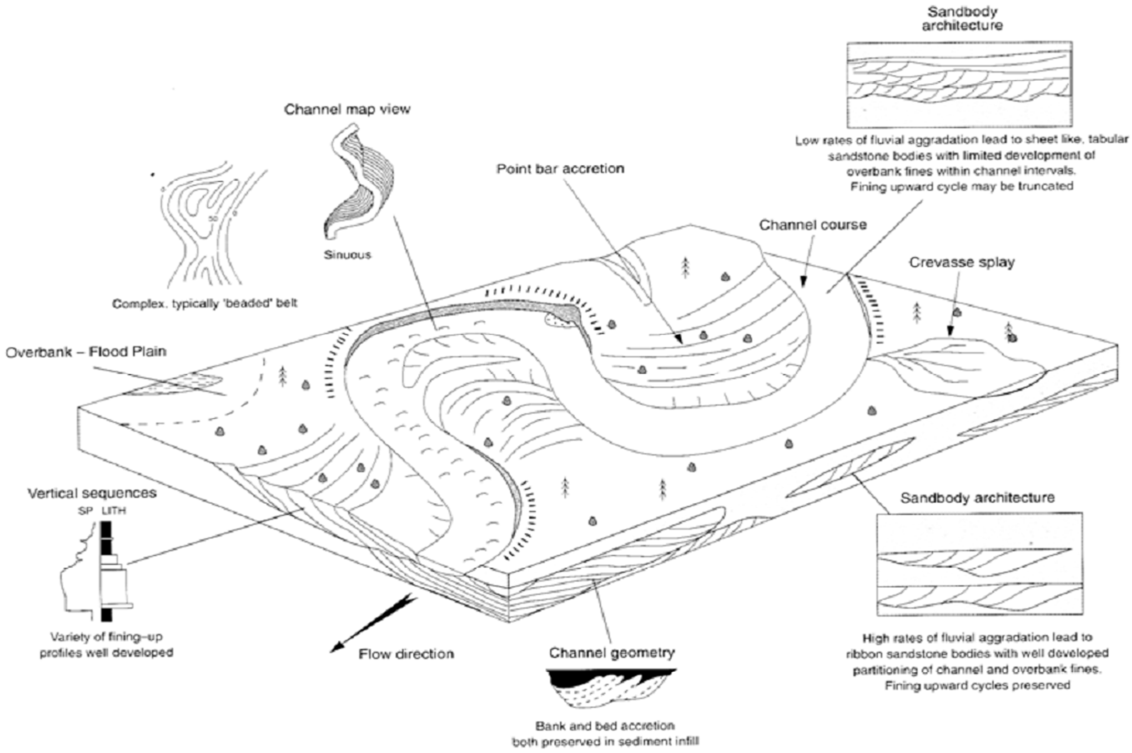

Figure 2 Block diagram of a high-sinuosity fluvial system illustrating the facies associations, channel belt and flood-plain sub environments. The point bar accretion is indicated. (C. Wiggers, 2009 after Emery and Myers, 1996)

A meandering river system deposited the Delft Sandstone member. At the time of deposition the West Netherlands basin was in an active phase of rifting. The top of the member consists of stacked sandstones. (Wiggers, 2009)

The principal reservoir sand bodies in the meandering system originate as point bars that are developed on the inner bank of meandering loops in response to lateral sand accretion (Donselaar & Overeem, 2008). In the gamma ray log the fluvial channels can be recognized by a fining upward log signature (DeVault & Jeremiah, 2002). Some minerals in the clay fraction are radioactive. The sand particles, mainly quartz, are not. In the courser quartz particles are gradually covered by smaller particles containing more clay minerals. In the gamma ray log this sequence can be seen as a gradual decrease of natural radiation with depth.

Based on the literature we can expect sand and silt deposits in the river channels. In the floodplains of the river a clay deposit is expected.

The member consists of a loose colourless, fine to medium grained, poorly sorted sub rounded to rounded sandstone and a light grey to dark grey, friable to firm siltstone. In between layers black to dark brown coal layers were deposited. Fossils shells and pyrite can be found within the layers.

<u>The Rodenrijs Claystone Member (SLDNR)</u>
The Rodenrijs Claystone Member was deposited in the Late Valanginian to the Early Hauterivian and was deposited in the western and central part of the West Netherlands Basin. It is interpreted as a lower coastal plain and a lagoonal deposition setting (DeVault & Jeremiah, 2002)It consists of a grey to light grey or white to crème white, friable siltstone. It has a loose colourless fine grained to medium grained, angular to sub angular, fairly sorted sandstone. The member has black to dark brown coal layers. The silty to sandy claystone in the member is light to medium grey.

<u>The Poseidonia Shale</u>

There is a possibility of finding oil in the Delft Sandstone member if the right trap structure is present. The main source of oil for the West Netherlands basin is the kerogen-rich marine shale from the Lower Jurassic. (Rondeel, Batjes, & Nieuweenhuijs, 1996). In this report the oil content of the Delft Sandstone member has been examined.

The reservoir

On top of the reservoir the literature study predicts a high shale content deposit. The Rodenrijs Claystone member consists mainly of clays from a lagoonal depositional environment. A lot of fossils can be found in this member.

Basedon the literature fluvial sediments in the reservoir section can be expected. These fluvial sediments would be mainly clay deposits in the floodplains and sand and silt deposits in the river channels and crevasse splays. Vegetation growing in the depositional environment has formed rare coal seams.

Beneath the Delft Sandstone member we can expect the sandy siltstones of the Alblasserdam member. These are fluvial deposits as well. A lot of claystone is to be found on the flood plains.

The Poseidonia Shale is a possible source rock. If a trap structure is present and mitigation and migration has occurred from this shale the reservoir may hold hydrocarbons.

Chapter 4 - Data and Methods

The study is based on the interpretation of data from the PNA-GT01 geothermal well in Pijnacker. The goal is to come up with a description of the reservoir content. To reach this goal an analysis of the cutting samples is performed. The results of this analysis is then correlated to the gamma ray log. This section describes the methods and sources of data used for this report.

Gathering of data while drilling

The drilling of the Geothermal well PNA-GT01 started at 9-3-2010 and was completed at 8-5-2010 at a total well depth of 2869,5 meters. The well is deviated and so the drilled depth is not the same as the true vertical depth. True vertical depth is the depth measured from the surface directly above a point.

The true vertical depth of the bottom of the well is 2229,5 meters. To optimise the drilling process and to gather data for new projects surveys are conducted while drilling a well.

Three surveys were conducted while drilling the PNA GT01 well:

- A gamma ray log. This is a measurement of the natural radiation of the rock drilled through. The result of this measurement is a plot of the gamma radiation measured in API against the drilled depth.
- A caliper log. The caliper log is a measurement of the size and shape of the borehole. The caliper log is plotted against the depth. caliper log was only conducted in the vertical part of the well.
- A collection of cuttings. At the drill bit rock is broken in fractions. These fractions are transported to the surface in a high density brine fluid called the drilling mud. At the surface the mud filtered at a vibrating machine called the shale shaker. Multiple screens separate the mud from the cuttings. At the shale shaker all the cuttings larger than 2mm are filtered out the mud. All cuttings larger than 2mm are filtered from the mud. The mud passing through is periodically collected by the drilling crew.

Figure 3 The Shale shaker in action at the Ammerlaan site

At the Ammerlaan drilling site cutting samples were collected from the reservoir section every 2,5 meters of drilled depth. The cuttings were collected as stated in the table.

Hole size(inch)	Interval, from – to(m AH-NAP)	Frequency
17 ½	0 – 60	None
12 ¼	60 – 1000	1 wet / 10m, 1 dry / 10m
8 ½	1000 – 2294	1 wet / 5m, 1 dry / 5m
6	2294 – 2576 (TD)	1 wet / 2.5m, 1 dry / 2.5m

Table 1 The collection of the cuttings as was performed during the drilling of PNA GT01 (Smeulders, 2010)

Processing and preparation of the cutting samples

Two types of cuttings are used for the examination. In this report they are referred to as the “wet” and the “dried” cuttings.

- The wet cuttings are the cuttings and mixed with drilling mud collected directly from the shale shaker. These cuttings contain all the grains smaller than 2mm. These cutting samples contain grains and the brine drilling mud.
  After collection these samples have been sealed in air tight bags and labelled.
- The dried cuttings are prepared from the wet cutting samples.
  - 100 ml of the wet cutting sample is used to prepare the dried cutting samples
  - The cuttings are flushed with fresh water to wash away the salt drilling mud.
  - The cuttings are sieved using a 1mm sieve and an 64µm sieve.
    - The grain fraction between 1mm and 2mm will be referred to as the <u>course cutting sample</u>
    - The grain fraction between 1mm and 64µm will be referred to as the <u>fine cutting sample.</u>
  - The sieved cuttings are then dried in an oven at 60°C. A higher temperature could destroy some minerals and hydrocarbons. When drying the cuttings a permeable cover protects the smallest particles from blowing away.

  After preparation the cuttings are stored in glass tubes and labeled.

Figure 4 An example of a wet cutting sample from the PNA GT01 well 2757,5m of drilled depth.

Cutting analysis

In this report the cuttings are visually analyzed using an optical stereo microscope. A description of every cutting sample from the reservoir interval was made.

- The main fractions of rock types are written down. An estimation of the volume percentage in the sample is made using the percentage estimation comparison charts by (Terry & Chilingar, 1955) and (Folk, Andrew, & Lewis, 1970).
- In the image analysis room at the TU Delft images were taken from different samples to support the report.
  17 images were made from different fine fraction cutting samples.
  9 images were made from different course fraction cutting samples.
- Grain size and rounding of the grains is estimated using a comparator card. This grain size comparator was originally designed by C. Jordan in 1974 for the American Stratigraphic institute.

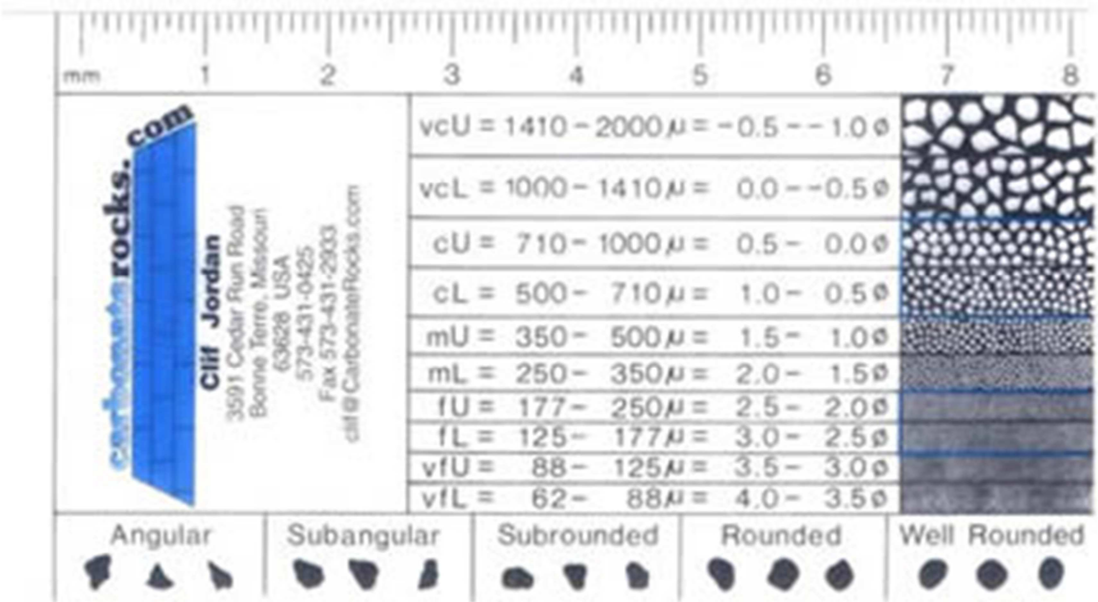

Figure 4 grain size comparator card example as it was used in the cutting analysis, example from carbonaterocks.com

Hydrocarbon content

Hydrocarbons fluoresce. So if oil is present in the cuttings this can be tested using ultraviolet light. Oils are exited using ultraviolet wavelengths (300-400nm) and fluoresce in the visible wavelength range (400nm-600nm) (TurnerDesign, 2007). Different types of oil emit different wavelengths. In the examination of the Ammerlaan cuttings under ultraviolet light the oil emits a yellowish green to orange light(550-620nm).

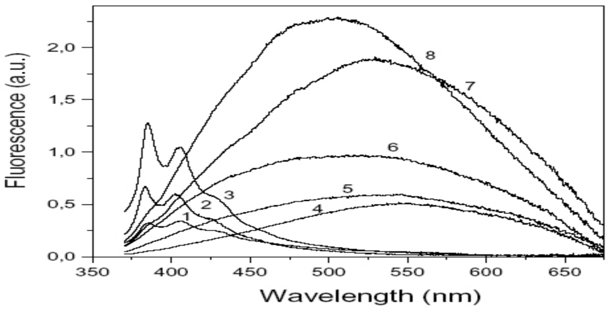

Figure 5 Wavelengths of visible light emitted by various types of oils (TurnerDesign, 2007)

1 – Motor oil
2 – Shell Diala oil
3 – Oil SAE 30
4 – Bunker Fuel oil
5 – Arabian Medium crude oil
6 – Basra crude oil
7 – German crude oil
8 – Nihian crude oil

The presence of oil in the cuttings of Ammerlaan was tested in the image analysis room at the TU Delft. In the test setup two powerful ultraviolet lights were installed above a black screen and the room was darkened.
Cutting samples in a petri dish were tested for hydrocarbon content under the ultraviolet light. An image was taken of every test using a camera installed above the setup.

Seven different wet cutting samples were investigated on fluorescence of oil.
Six dried cutting samples were investigated.

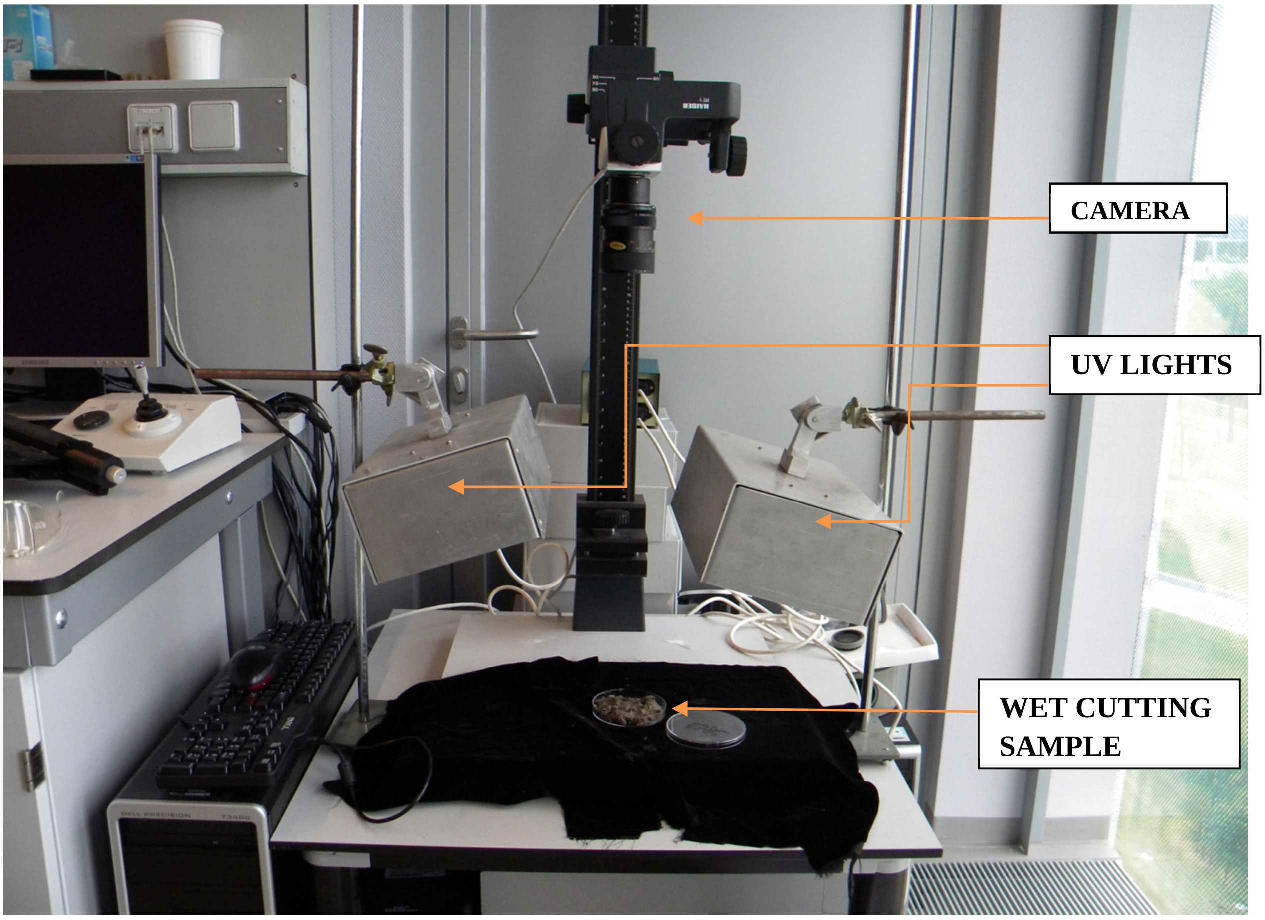

Figure 5 The set-up for determining hydrocarbon content of wet cuttings using ultraviolet light

Gamma ray log interpretation and correlation to the cutting samples

The gamma ray log shows the natural gamma ray emitted from the rock. Shale containing silt and claystones are naturally higher in radiation than sandstones. The gamma radiation is a measurement of the shale content.

Due to compaction of the formation the shale content from the gamma ray needs a correction. The Old Rock equation corrects for the compaction. According to Larionov(1969) for Mesozoic rocks the shale volume can be calculated from the gamma ray log:

- $V_{shgr} = \frac{GR_{log} - GR_{min}}{GR_{max} - GR_{min}}$ *shale volume from gamma ray*
- $V_{sh} = 0.33 \times (2^{2 \cdot V_{shgr}} - 1)$ *Old Rock equation for Mesozoic rocks*
- The Sandstone line GRmin is at 15 degrees API
- The Shale line is chosen at 130 degrees API

The shale point of 130 degrees cannot be found in the Delft Sandstone Member. In the cutting examination all the intervals contain an amount of quartz. In the Rodenrijs Claystone member a clay layer occurs at 2692 meters of drilled depth. This point is taken as the shale point.

In the log interpretation both the gamma ray and the shale content are shown per interval together with one or multiple images of the cuttings. The images were taken at the image analysis room at the TU Delft.

Flow chart of cutting analysis from collection to implementation

For practical use in future studies the methods above are summarized in a flow chart. The chart describes how the cutting analysis process schematically was conducted in this analysis.

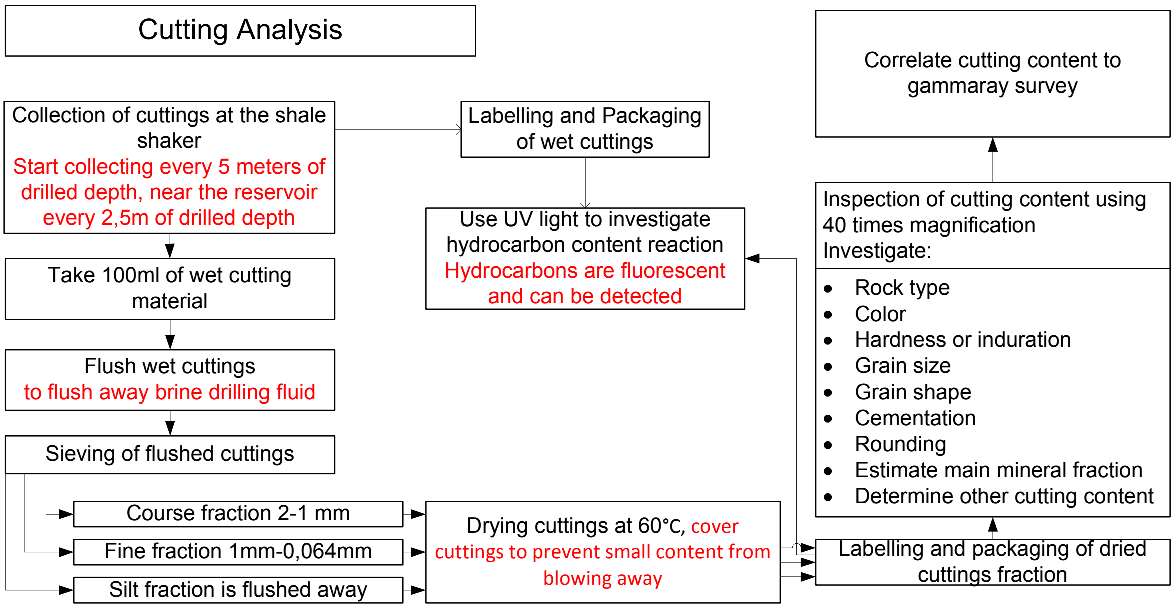

Figure 6 Flow chart of cutting collection, processing and implementation as was used for this report

Chapter 5 - Cutting content and grain size estimation with XRF and Microscope

The study on the regional geology concluded that the Delft Sandstone Member is a fluvial deposit in a lower coastal plain. (Bogaeart & Kouwe, 1993). When the production of the wells started samples were taken of the produced water. This water contained elements from the reservoir. Most of the grains are from the silt fraction. The mineralogical content of these grains should resemble the grain content of the actual reservoir.

The mineralogical content of the grains has been studied by using a XRF analysis. (De Leeuw & Langeveld, 2010). XRF is a method to determine the weight percentage of elements as a fraction of the total weight of the sample.

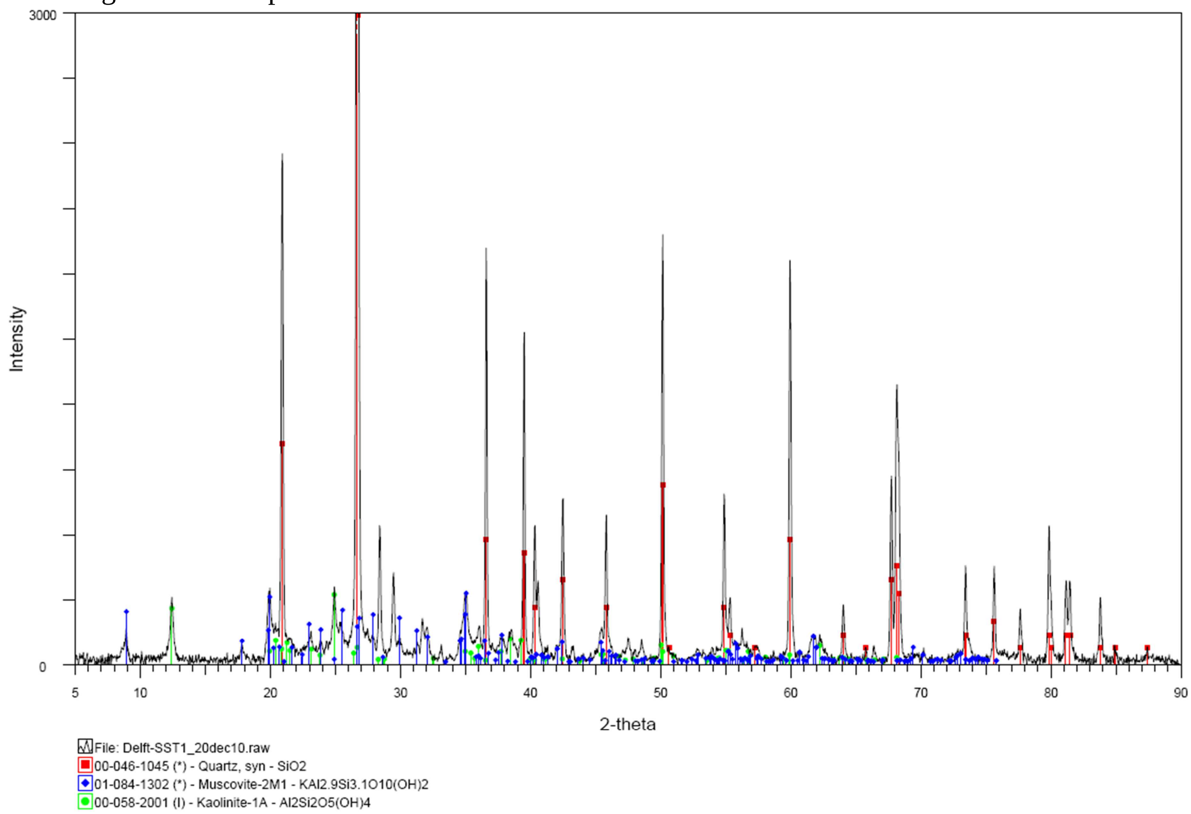

Figure 7 The result of the XRD analysis (Langeveld and de Leeuw, 2010)

From this XRF analysis the weight percentage of the occurring elements can be calculated. Every peak in the figure above resembles one element. The intensity of the peak is a measure for the weight percentage of an element in the sample. The weight percentages of different elements from this test are given in the table.

These elements occur in minerals in the grains. It is possible to determine to calculate the minerals formed by these elements using a software program.

Elements	wt%	StdErr
+SiO2	72,47	0,50
+Al2O3	14,46	0,23
+K2O	3,78	0,21
+CaO	2,58	0,18
+Fe2O3	2,31	0,17
+Cl	1,74	0,15
+Na2O	0,799	0,088
+TiO2	0,731	0,081
+MgO	0,519	0,057
+S	0,233	0,012
+P2O5	0.052	0.002
+MnO	0.0219	0.0014

Table 1 Elements found in the solid material produced with the water of the Ammerlaan well using XRF, revised after (Langeveld and de Leeuw, 2010)

Minocomp is a computer program written by K.H.A.A. Wolf, TU Delft to determine the volume percentage of minerals from the oxide percentages of elements. In steps it works as follows:

1. First the mol fraction of the elements is determined from the weight percentages.
2. A weight loss percentage is determined. In the preparation of the sample some loss of weight occurs.
3. All the Oxygen and Carbon molecules are considered weight loss.
4. The computer program provides a list of twenty common minerals in sedimentary rocks. The elements will be divided among these minerals based on their mole fraction. One mineral has to be selected a time and all the elements composing this mineral are deleted from the list of elements. Thus step by step all the elements are divided among minerals. All the carbon and oxygen molecules needed for some minerals are constructed from the weight loss percentage.
5. The elements that occur in only one mineral in the database are chosen first.
   The order in which the minerals were chosen:
   a. Halite
   b. Rutile
   c. Ca-Apatite
   d. Pyrite
   e. Muscovite
   f. Kaolinite
   g. Calcite
   h. Siderite
   i. Magnesite
   j. Quartz
6. The program has divided all the elements among the minerals and presents a list of mole percentage, weight percentage and volume percentage.

Mineral	Chemical formula	Mole %	Weight %	Volume %
Muscovite	$\mathbf{KAl_2[(OH,F)_2\|AlSi_3O_{10}]}$	0,071	0,311	0,301
Kaolinite	$\mathbf{Al_4[(OH)_8\|Si_4O_{10}]}$	0,019	0,053	0,056
Calcite	$\mathbf{CaCO_3}$	0,040	0,044	0,044
Magnesite	$\mathbf{MgCO_3}$	0,012	0,011	0,010
Siderite	$\mathbf{FeCO_3}$	0,022	0,028	0,020
Quartz	$\mathbf{SiO_2}$	0,821	0,539	0,558
Pyrite	$\mathbf{FeS_2}$	0,003	0,004	0,002
Rutile	$\boldsymbol{TiO_2}$	0,008	0,007	0,005
Ca-Apatite	$\mathbf{Ca_5[(F,OH,Cl)\|(PO_4)_3]}$	0,000	0,001	0,001
Halite	$\mathbf{NaCl}$	0,004	0,002	0,003
Total	-	1	1	1

Table 2 Mineral content calculated from the weight percentage measured in the XRF

The volume of the grains produced with the warm water of the Delft Sandstone member consists mainly of Muscovite and Quartz. Muscovite can be found in claystone. Quartz is the main component of the sandstone. Both claystone and sandstone deposits were expected in the fluvial depositional setting.

The volume percentage of these elements is the percentage in the produced water. Small particles, like clay particles containing the Muscovite are transported more easily by the water than courser sand particles. This has an effect on the percentages shown above. In the actual reservoir it is not unlikely to find a lower muscovite percentage.

Chapter 6 - Sample description of GT01 Delft Sandstone member and correlation to gamma ray using 3 characteristic intervals

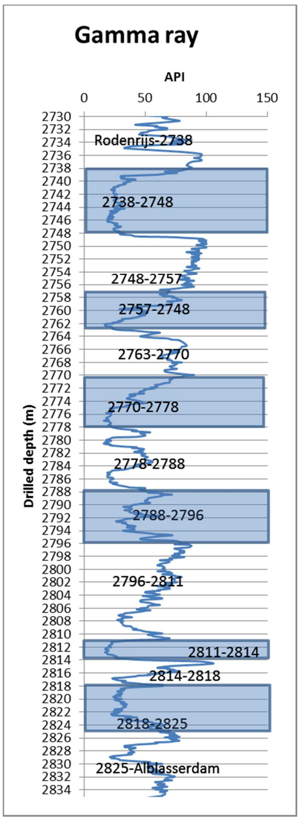

Table 3 The intervals as they were grouped and the Gamma ray log from the PNA GT01 well

The interval of the Delft sandstone in the GT01 PNA well is 2738 to 2825 meters of drilled depth. This is 2138 to 2209 meters of actual depth from the surface.

The cutting samples will be correlated to the gamma ray log. The reservoir has been divided in to thirteen sections. In the figure to the right the different intervals are shown.
The Shale content can be estimated from the gamma ray log. For every interval the shale content and the gamma ray log are plotted as a function of depth.

The intervals are supported by images. The main components of a cutting sample are numbered and a legend names the grains. A short text describes the interval. In the appendix a detailed descriptions of all samples is presented.

This chapter describes three distinguishable intervals found in the Delft Sandstone member on the basis of their cutting samples and the gamma ray log.

- A sandstone cutting sample. 2738-2748
- A fining upwards sequence. 2770-2778
- A claystone cutting sample. 2748-2757

Interval 2738 – 2748

The top of the Delft Sandstone member is a 10meter thick sandstone layer. High quartz content can be found in the cutting samples of this interval of 35% to 50%. Cement traces are visible on the quartz grains. The majority of the silt fraction was flushed.

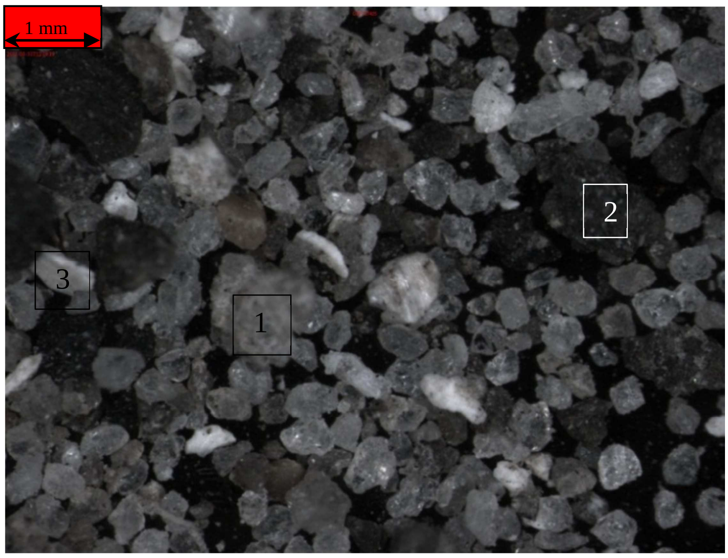

Figure 6 GT01 PNA 2742,5 fine fraction (,064-1mm) dried cutting sample The scale bar in the top left depicts 500microns.

1. Quartz with cement
2. Claystone
3. Calcite

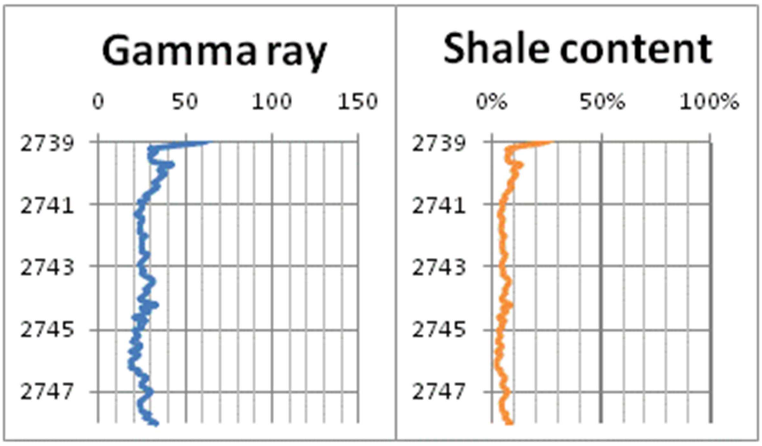

Figure 7 gamma ray log in API and Shale content in volume percent from the interval 2739m-2747m of the PNA GT01 well

The first selected interval of the Delft Sandstone member is a sand deposit of 10 meters in thickness.

This interval consists for 95% out of non-shale content.

Interval 2770-2778

In the gamma ray log of this interval a decrease of radiation is visible. This could be a fining upwards sequence. At the top of this sequence one could expect a lot of very fine to silt material, such as a siltstone or a claystone.

In the cuttings the sample from the top of the structure shows a higher siltstone and claystone content. The quartz grains are in estimation using the comparator card smaller than the grains found deeper in the sequence. The quartz content of the cuttings increases with depth in this sequence. This interval can be interpreted as a fining upward sequence.

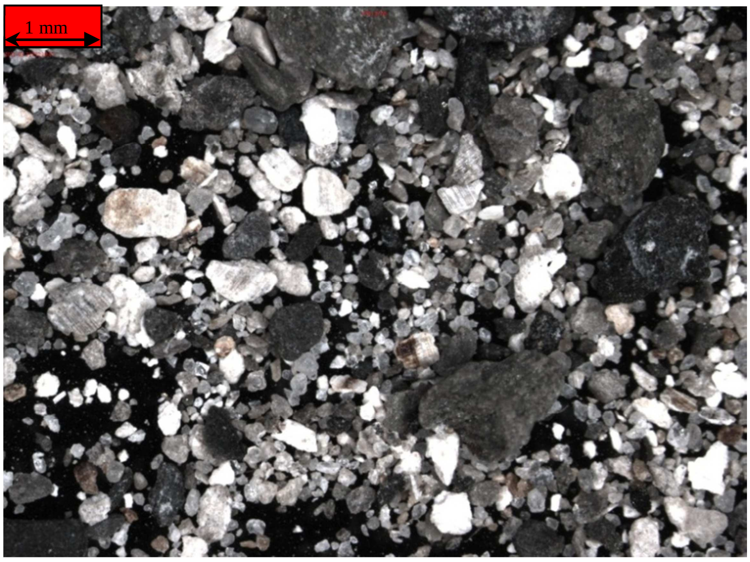

Figure 8 GT01 PNA 2772,5 fine fraction(0,064mm-1mm) dried cutting sample. The scale bar in the top left depicts 500microns.

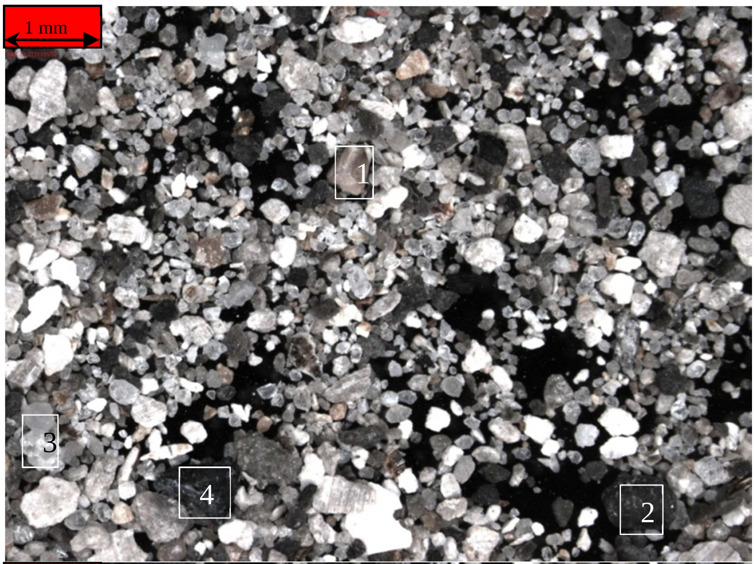

Figure 9 GT01 PNA 2775 fine fraction (0,064mm-1mm) dried cutting sample The scale bar in the top left depicts 500microns.

1. Calcite
2. Grey Claystone
3. Quartz
4. Coal

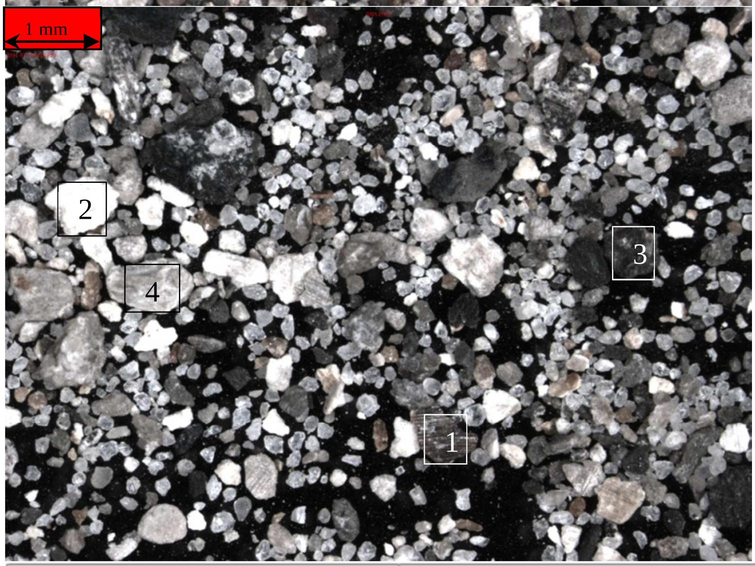

Figure 10 GT01 PNA 2777,5 fine fraction(0,064mm-1mm) dried cutting sample
The scale bar in the top left depicts 500microns.

1. Layered Calcite
2. Cemented Quartz
3. Dark grey siltstone
4. Light grey claystone

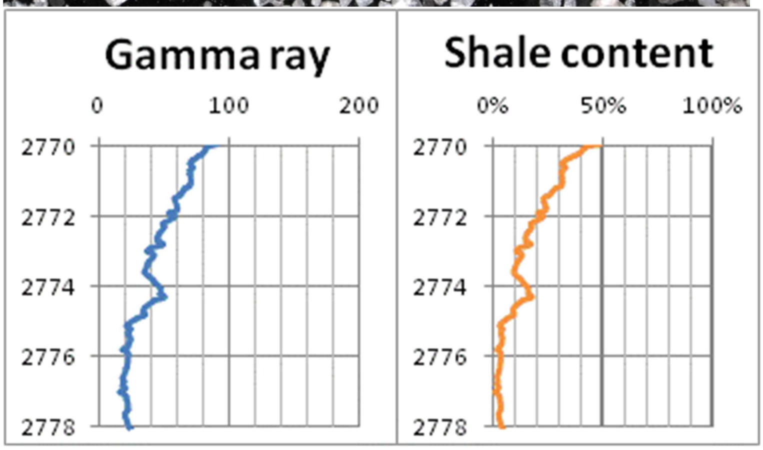

Figure 11 gamma ray log in API and Shale content in volume percent from the interval 2770m-2778m of the PNA GT01 well

This interval shows the gradual decrease in natural radiation and so in shale content. This can be interpreted as a fining upward sequence found in point bars in fluvial deposits.
A Quartz grain size increase is visible. Though this needs further tests. (Recommendations)

Interval 2748- 2757

In the middle of this interval at 2752,5 meters of drilled depth the fine fraction contains a lot of quartz grains. At least 50% of the grains in this sample are quartz. The gamma ray predicts a shale volume percentage of 50% at this depth.
The cuttings hold material from the fractured rock at the drill bit, but they also hold material from

caving above the drill bit. This could cause the high quartz content of this cutting sample. Another explanation for the low shale content of this sample is the flushed silt fraction.
The course fraction contains approximately 45% claystone.

Figure 12GT01 PNA 2752,5 fine fraction (0,064mm-1mm) dried cutting sample. The scale bar in the top left depicts 500microns.

1. Coal
2. Dark Grey Siltstone
3. Quartz (no cement)

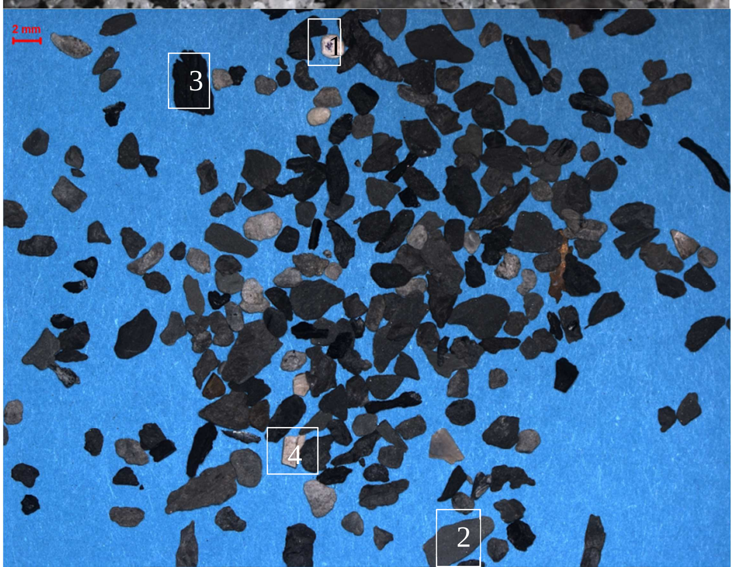

Figure 13GT01 PNA 2752,5 course fraction (1mm-2mm) dried cutting sample. The scale bar in the top left depicts 2mm.

1. Cemented Quartz
2. Medium grey Claystone
3. Coal
4. Calcite

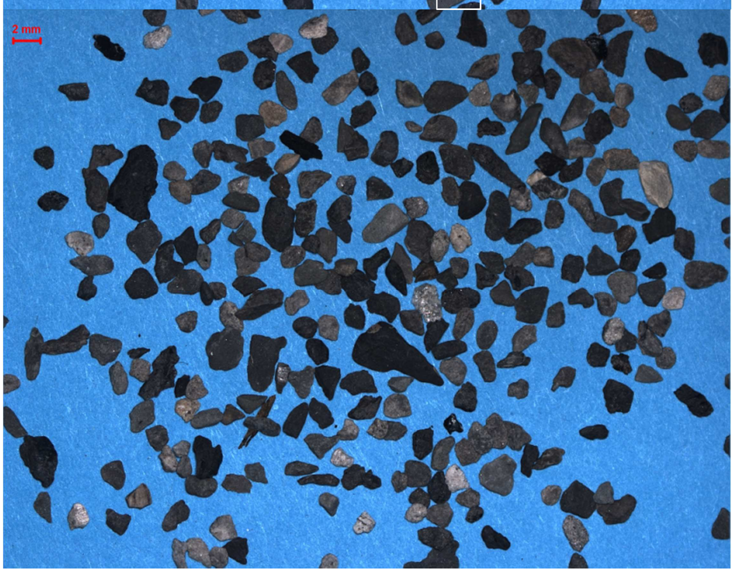

Figure 14GT01 PNA 2750 course fraction (1mm-2mm) dried cutting sample. The scale bar in the top left depicts 2mm.

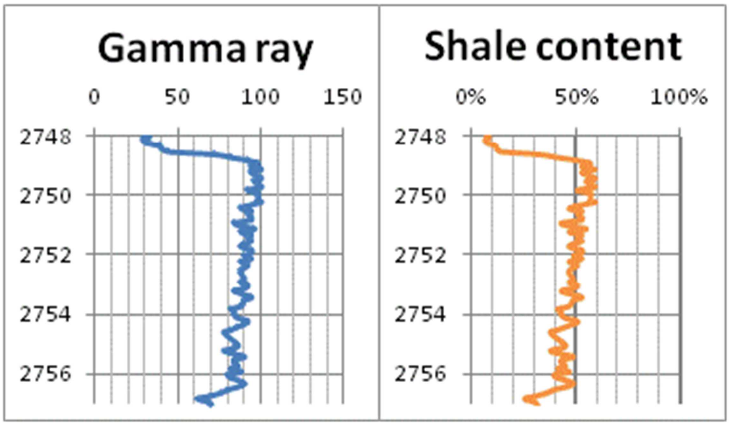

Figure 15 gamma ray log in API and Shale content in volume percent from the interval 2748m-2757m of the PNA GT01 well

The second chosen interval shows a high shale volume percentage of 50% in average. This increases the gamma ray log. It still has a lot of quartz in the fine fractions.

Chapter 7 - Hydrocarbon content

The dried cuttings were examined first by using the setup discussed in chapter 4. Some grains lit up green, to orange when they were placed under the ultraviolet light. The result was not satisfying; it was too hard to see noticeable colour changes with the naked eye.
To confirm the presence of hydrocarbons the wet cuttings were tested next. These cuttings did not show a clear enough emission of light when examined by the naked eye. The green orange glow could be observed. But the images taken from these samples showed very clear bright tracks.

Cutting samples taken from different depths in the reservoir were examined. All of these contained hydrocarbons. As a check one cutting sample from the Rodenrijs Claystone was examined. Nothing in this sample reacted to the ultraviolet light.

Using ultraviolet light to test for hydrocarbon presence is a qualitative check. It is not possible to predict the amount of hydrocarbons present in the reservoir from this test result.

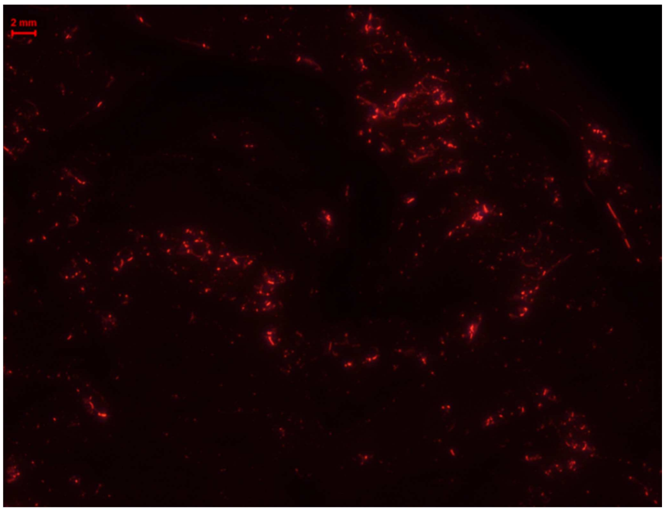

Figure 16 GT01 PNA 2745 wet cutting sample under UV light. The scale bar in the top left depicts 2mm.

This is the first sand interval 10 meters in thickness at the top of the Delft Sandstone group. Under UV light hydrocarbons emit visible light. The emitted light can be seen on the image in red. When viewed on eyesight the emitted light was yellowish green to orange.

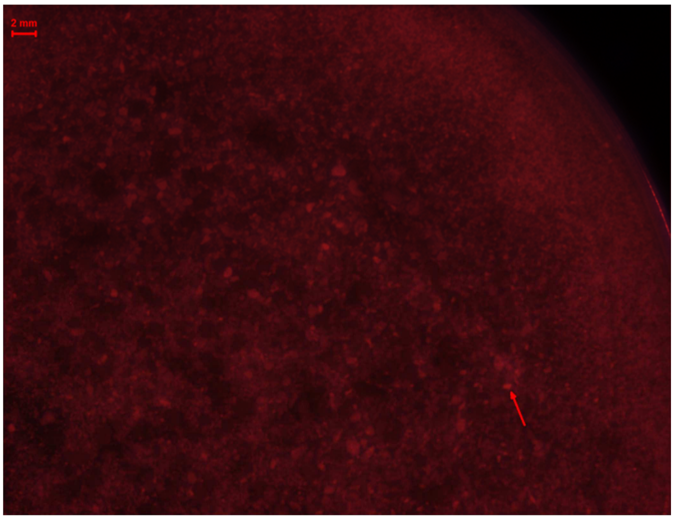

Figure 17 GT01 PNA 2777,5 dried cutting sample under UV light. The scale bar in the top left depicts 2mm.

The image shows a dried cutting sample illuminated by ultraviolet light. Some grains have hydrocarbons attached to them. These grains light up. The bright red spots are the grains covered in oil. To the eye the grains the hydrocarbons emit a yellowish green to orange light.

Chapter 8 - Results of correlations

This chapter summarizes the findings of the cutting analysis. The analysis resulted in an overview of the types of rock in the cutting samples and an estimation of the proportion of each type of rock. An estimation of the grain size was made. And from the Gamma ray log the shale content was calculated. These results are plotted together on the following page. Fluorescence analysis resulted in the proof of hydrocarbons in the rock.

From the cutting analysis an estimation of the content of the reservoir can be made. Every cutting sample was examined using a stereo microscope. Most of the cuttings consist of the same main grains; Sandstone, Siltstone, Claystone and Coal. Traces of calcite and fossils are found. Siderite and pyrite minerals are found in the cuttings.

However, in some high radiation intervals shown in the gamma ray log the cuttings contain a lot of quartz grains. A lower natural radiation would be expected. The reason for this mismatch could be the flushed silt fraction, this fraction was not analyzed. Another reason for the mismatch is a mixing of caving and cutting grains in the sample.

The grain size was estimated by using the stereo microscope and a grain size comparator card. This rough method is not sufficient to clearly find the fining upward sequences in the size of the quartz grains in the Delft Sandstone member. These sequences are expected when the method of deposition is a fluvial deposit. The figure gives a representation of the grain size distribution. Rough differences in size are measurable using the comparator card. In a follow up analysis of the grain size a better graph should be possible. (Recommendations)
The cutting content does show a difference in grain type. More silt- and claystones are found in the top of the fining upwards structures and more quartz grains are found in the bottom of these structures. Two fining upward structures are present in the reservoir section.

Cutting inspection under ultraviolet light proved the presence of oil throughout the reservoir. Both dried cuttings and wet cuttings were analyzed. To the naked eye the yellowish orange glow exited from the hydrocarbons is better visible. However the images created by the camera show clearer results for the wet cutting samples; the emitted light is brighter for these samples.

The boundary between the Alblasserdam member and the Delft Sandstone member can be determined on the fossil content of the cuttings. The Alblasserdam contains a type of shell not seen in the cuttings from the Delft Sandstone member.
The following page shows the gamma ray log, the cutting content, the grain size and the shale content in the reservoir section of the PNA GT01 well.

The gamma ray log, cutting content estimation, grain size and the shale content of the PNA GT01 well

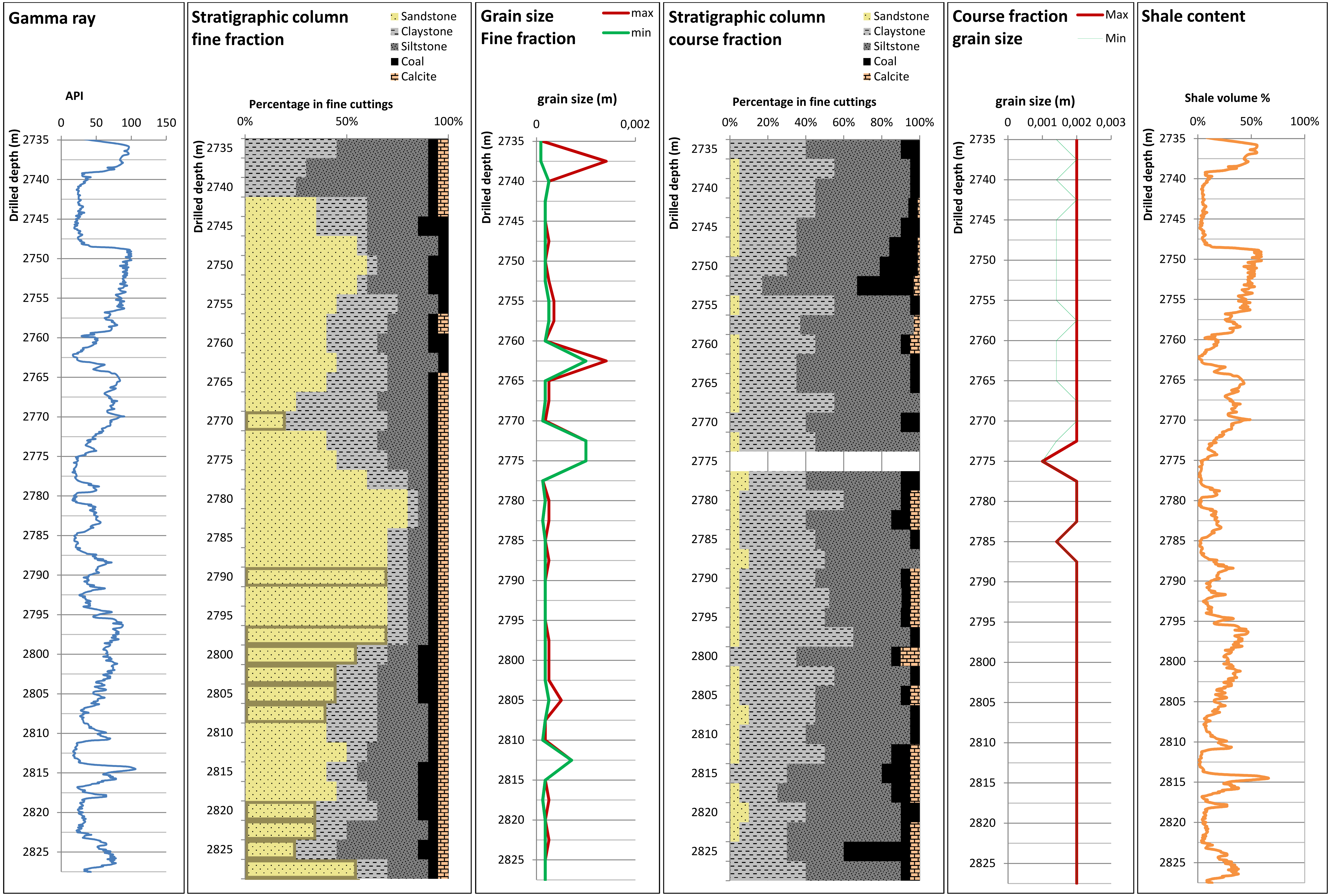

Shale content from gamma ray	Images of hydrocarbon, throughout the reservoir.	Stratigraphic column	Full scale width of an image is 7cm	Drilled depth cutting image

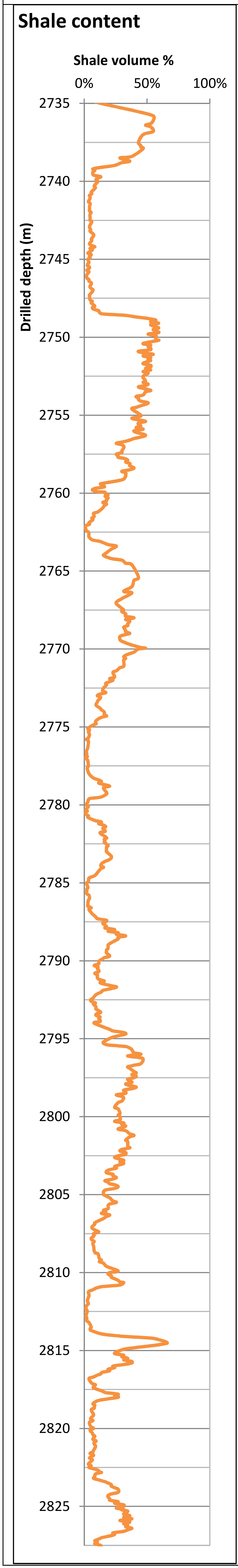

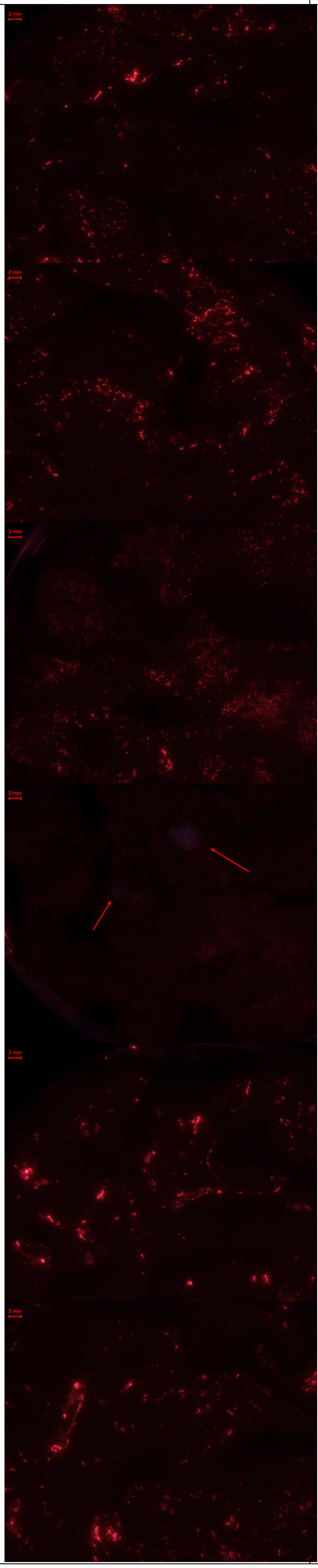

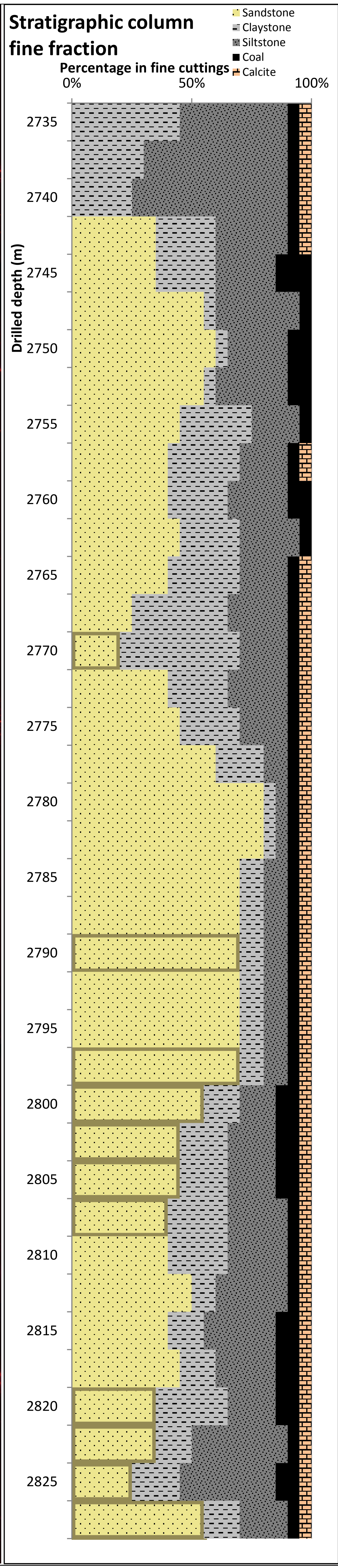

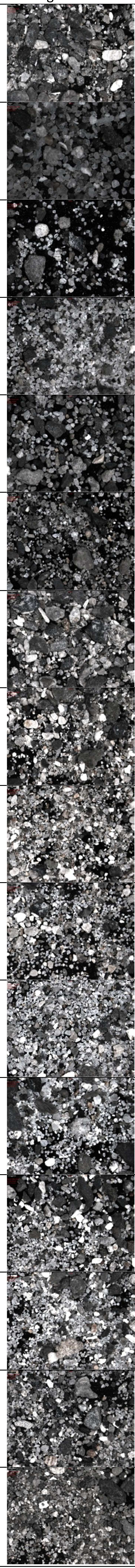

GT01 2735
GT01 2742,5
GT01 2745
GT01 2752,5
GT01 2757,5
GT01 2760
GT01 2770
GT01 2772,5
GT01 2775
GT01 2777,5
GT01 2785
GT01 2795
GT01 2812,5
GT01 2815
GT01 2825
GT01 2830

Chapter 9 – Discussion and Conclusions

The Delft Sandstone member is a fluvial deposit from the Late Jurassic to Early Cretaceous. In Pijnacker the member is used as a geothermal water reservoir by Ammerlaan. The PNA GT01 well drilled for this project produces warm water from this reservoir. At the well location the layer has a true vertical thickness of 66 meters.

An estimation of the content of the cutting samples is presented. The main fractions in the cuttings are provided in a graph. However these cutting samples have a disadvantage.
Caving material taken up from the borehole wall by the mud stream will mix with the cuttings detached from the rock by the bit. And so the cuttings might be a blend of multiple layers.
In the preparation of the dried cuttings for this report the silt fraction was flushed. This may result in a distorted representation of the reservoir.

The main minerals found in this reservoir are Muscovite and Quartz, this was determined using a XRF analysis. In cutting samples collected while drilling the PNA GT01 well claystone, sandstone, siltstone and coal are the most common fractions. Pyrite and Siderite minerals and fossil shells are found in the reservoir cuttings.

The content of the fine cutting samples is in line with the gamma ray log. This was not really the case for the course cutting samples. All the course fractions are mainly composed of the dark grey siltstone and the light grey claystone. Variations in sandstones were not noticeable in the course cutting fractions. In future examinations it is suggested to examine the smaller fraction.

The gamma ray log shows sand layers as zones of low natural radiation. Some of these layers are loose friable sandstone and some of them consist of cemented quartz grains. In reservoir models this cementation might have to be considered since it can have an impact on permeability (Manmath & Lake, 1995)

Fining upward sequences in the gamma ray and an increase in quartz grain size in the cuttings can be implemented as point bar systems. This would confirm the Delft Sandstone Member to be a fluvial deposition.

All the sand layers in the member at the GT01 site contain hydrocarbons.

Recommendations

In future research projects on cuttings the silt fraction should be collected during the sieving proces. It might be possible to collect it using filter paper (even a coffee filter would suffice).

If there is a possibility for future wells to collect core samples this is recommended. Permeability and porosities could then be measured. This is of course an extra expense.

In cutting analysis if there are course and a fine fraction samples available first examine the fine fraction first. In this report more details were find in this fraction.

The grain sizes of quartz could be measured and used in the Karman-Kozeny equation to determine the permeability. Porosities of the reservoir can be estimated using this relation and Delft-03 cuttings.

The GT01 well was studied for this report; a similar study of the GT02 well would increase the understanding of the Delft Sandstone Member.

If new geothermal wells are drilled in the Delft area and cuttings are available a fluorescence test should be conducted at an early stage to determine possible hydrocarbon content. This is an easy set-up experiment.

For further understanding of the hydrocarbon content of the Delft Sandstone member a quick test of hydrocarbon content in the PNA GT02 cuttings would be recommended.

Acknowledgements

For the all the help with the project as a supervisor, his feedback on the report and his assistance in the implementation of the XRF data I would like to thank Karl-Heinz Wolf.
Joost van Meel helped me with the images taken in the Image Analysis room at the TU Delft. Remco Groeneberg was very helpful in the start up of the project; I would like to thank him for the help with the gamma ray log and his overall assistance. Rick Donselaar helped me with the microscope and the analysis of the cuttings.
From PGMI I would like to thank Julien Smeulders, the well geologist of the PNA-GT01 well. He provided me with the dried cutting samples and the well data.
Furthermore I would like to thank Ammerlaan for the visits, their explanation of the doublet and the wet cutting samples.
I would also like to thank Chris den Boer for his aid in collecting the cuttings from the drilling location at Pijnacker.

References

Bogaeart, v. A., & Kouwe. (1993). *Stratigraphic nomenclature of the Netherlands.*

De Jager, J., Doyle, M., Grantham, P., & Mabillard, J. (1996). Hydrocarbon habitat of the West Netherlands Basin. In H. Rondeel, D. Batjes, & W. Nieuwenhuijs, *Geology of gas and oil under the Netherlands* (pp. 191-209). Dordrecht: Kluwer Academic Publishers.

De Leeuw, L., & Langeveld, J. (2010). *Sandstone quality for geothermal use: Delft Sandstone from the Ammerlaan wells.* Delft: TU Delft.

DeVault, B., & Jeremiah, J. (2002). Tectonostratigraphy of the Nieuwekerk Formation (Delftland Subgroup), West Netherlands Basin. *AAPG Bulletin* , pp. 1679-1707.

Donselaar, M., & Overeem, I. (2008). Connectivity of fluvial point-bar deposits: An example from the Miocene Huesca fluvial fan. *AAPG Bulletin* , pp. 1109-1129.

Drost, G., & Korenromp, M. (2010). *Sediment petrographical analysis of the Delft Sandstone.* Delft: BSC thesis, Delft University of Technology.

Folk, R., Andrew, P., & Lewis, W. (1970). Detrital sedimentary rock classification and nomenclature for use in New Zealand. *New Zealand Journal of Geology and Geophysics* , 937-968.

Gilding, D. (2010). *Heterogeneity determination of the Delft subsurface for heat flow modelling.* Delft: Msc Thesis, TU Delft.

Manmath, N., & Lake, L. (1995, March). A physical model of cementation and its effects on single-phase permeability. *AAPG Bulletin* , pp. 431-443.

Rondeel, H., Batjes, D., & Nieuweenhuijs, W. (1996). *Geology of Gas and Oil under the Netherlands.* The Hague: Springer.

Smeulders, J. (2010). *Drilling Program Pijnacker Geotherma-01 (PNA-GT01).* Groningen: PGMI BV.

Smits, P. (2008). *Construction of an integrated reservoir model using the Moerkapelle field for geothermal development in the Delft Sandstone.* Delft: Msc Thesis, TU Delft.

Terry, R., & Chilingar, G. (1955). Summary of 'Concerning some additional aids in studying sedimentary formations' by M.S. Shretsor. *Journal of sedimentary petrology* , 229-234.

TurnerDesign. (2007, March). What is crude oil - http://www.turnerdesigns.com/t2/doc/appnotes/S-0079.pdf. Sunnyvale, California, United States of America.

Van Balen, R., F., V. B., De Leeuw, C., Pagnier, H., Simmelink, E., Verweij, H., et al. (2000). Modelling the hydrocarbon generation and migration in the West Netherlands Basin, The Netherlands. *Journal of Geochemical exploration* , 685-688.

Wiggers, C. (2009). *The Delft Sandstone in the West Netherlands Basin.* Delft: Delft University of Technology.

Wong, T. E. (2007). Jurassic. In T. Wong, D. Batjes, & J. De Jager, *Geology of the Netherlands* (pp. 107-125). Royal Academy of Arts and Sciences.

Supplementary data

<u>How to use this chapter:</u>

- Every interval has a short description
- An estimation of the cutting content is given for the fine fraction
- A picture of the fine and/or course fraction is presented, typical grains are pointed out
  In the left upper corner of the pictures a ruler depicts the scale. Typically a picture has a full scale size of 7cm.
- The gamma ray of the section is presented
- The shale content derived from the gamma ray is presented

Interval Rodenrijs Claystone-2738

This interval is described to give a clear top of structure of the Delft Sandstone member. The Delft Sandstone starts at the top of the first sand layer of 10 meters in true vertical thickness. This description holds only for the Delft Sandstone used for the GT01 and GT02 wells.

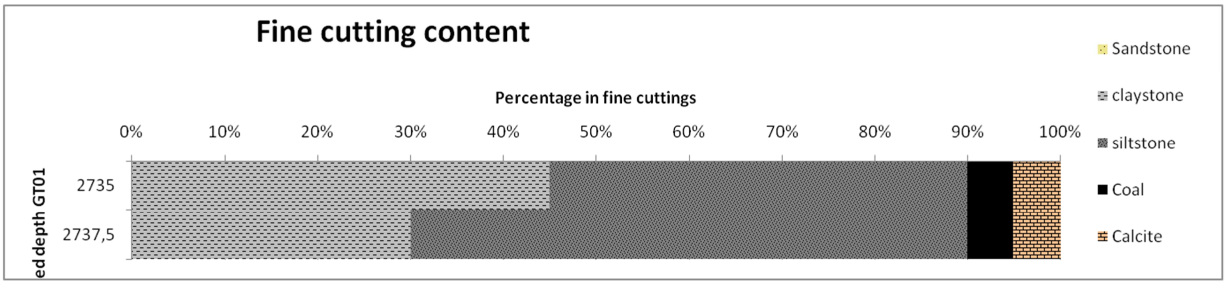

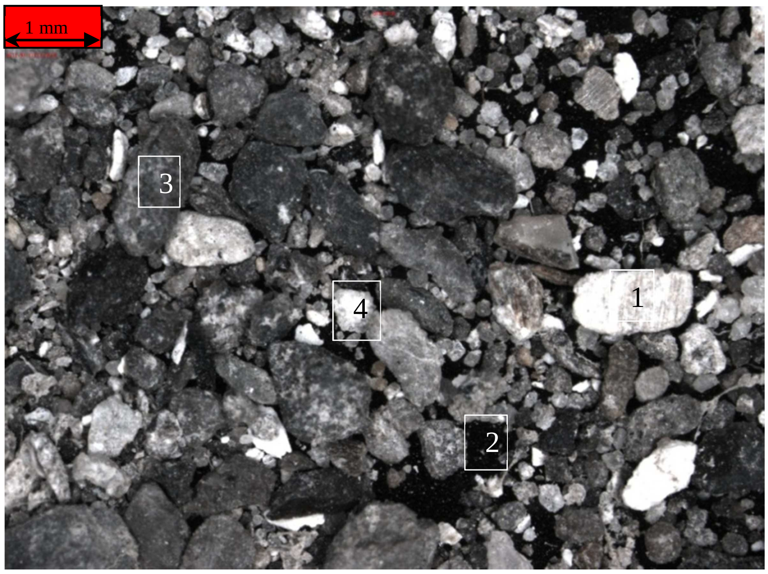

Figure 18 GT01 PNA 2735 fine fraction (0,064-1 mm) dried cutting sample.

Cutting sample content:

1. Laminated calcite
2. Lignite particle
3. Dark grey claystone
4. Cemented Quartz

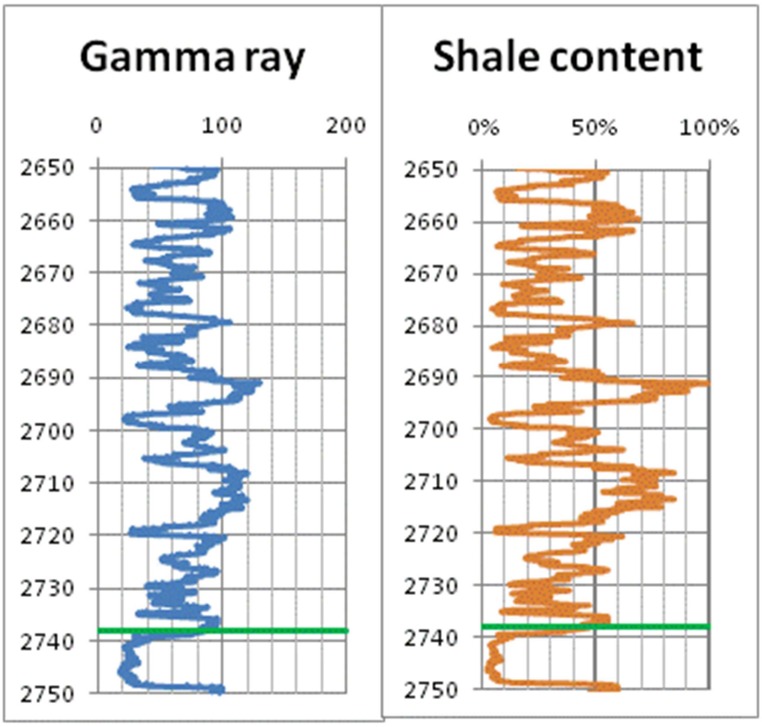

Figure 19 gamma ray log in API and Shale content in volume percent from the interval 2650m-2750m of the PNA GT01 well

The Rodenrijs Claystone member is a stacking of silty to sandy clay layers with coal layers of a maximum thickness of 2 meters in between clay layers.
The member has a typical saw tooth pattern.
The green line in the pictures indicates the top of the Delft Sandstone member. It starts at the top of the first sandstone deposit of more than 10 meters for the GT01 and GT02 wells.

Interval 2738 – 2748

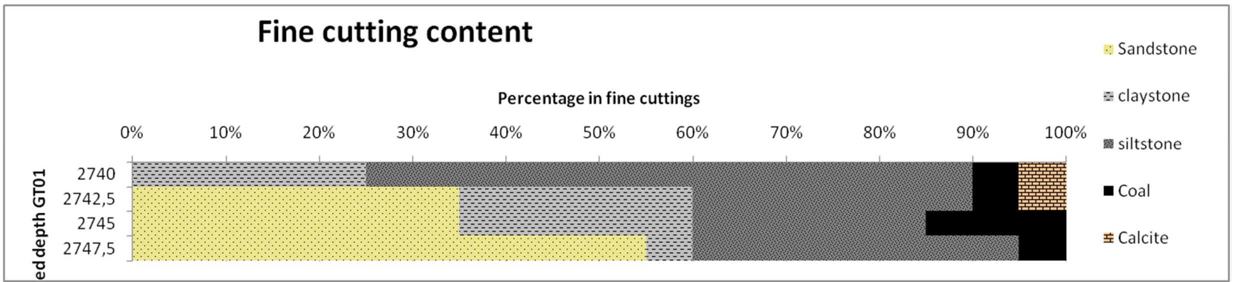

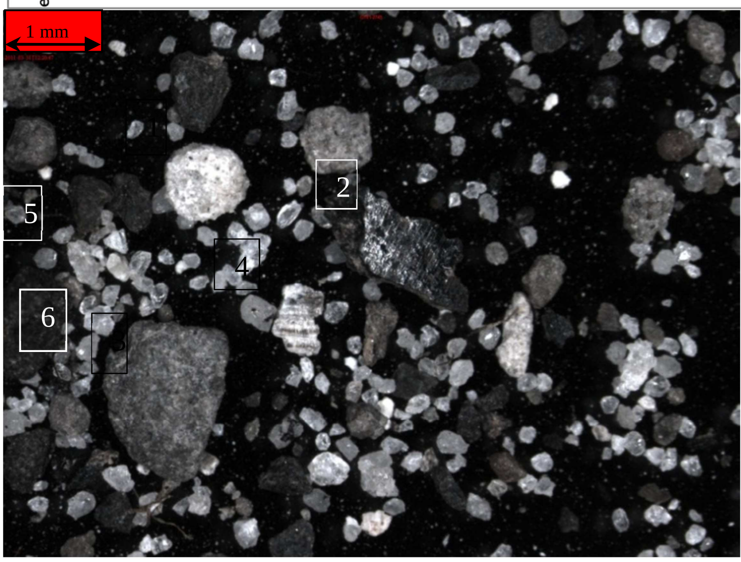

Figure 20 GT01 PNA 2745 fine fraction (0,064-1 mm) dried cutting sample.

1. Cemented Quartz
2. Coal
3. Grey Claystone
4. Layered Calcite
5. Quartz
6. Dark grey siltstone

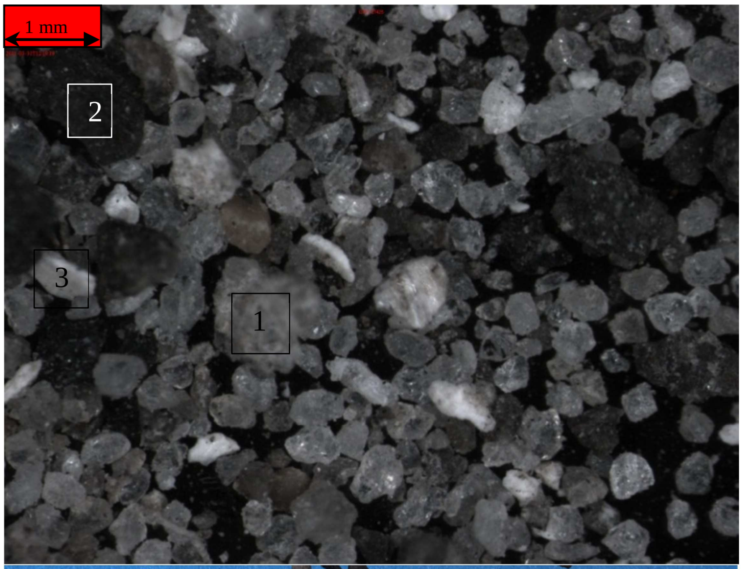

Figure 21 GT01 PNA 2742,5 fine fraction (,064-1mm) dried cutting sample.

1. Quartz with cement
2. Dark grey siltstone
3. Calcite

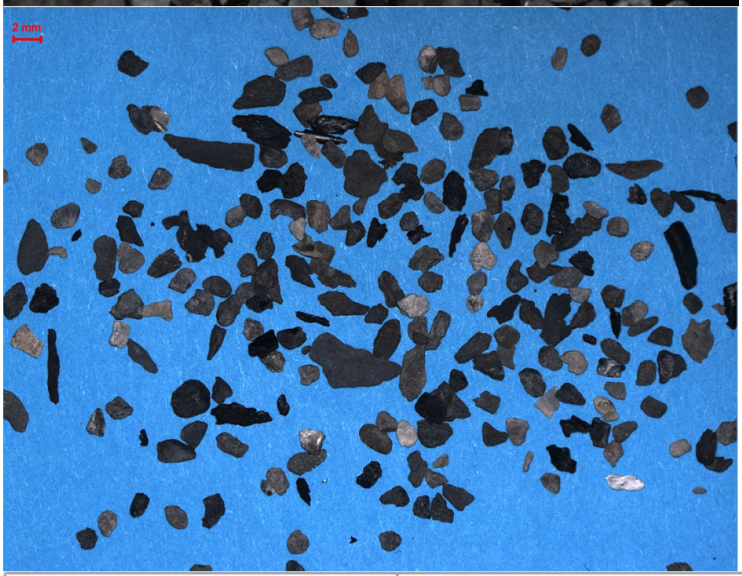

Figure 22GT01 PNA 2742,5 course fraction (1mm-2mm) dried cutting sample. The scale bar in the top left depicts 2mm.

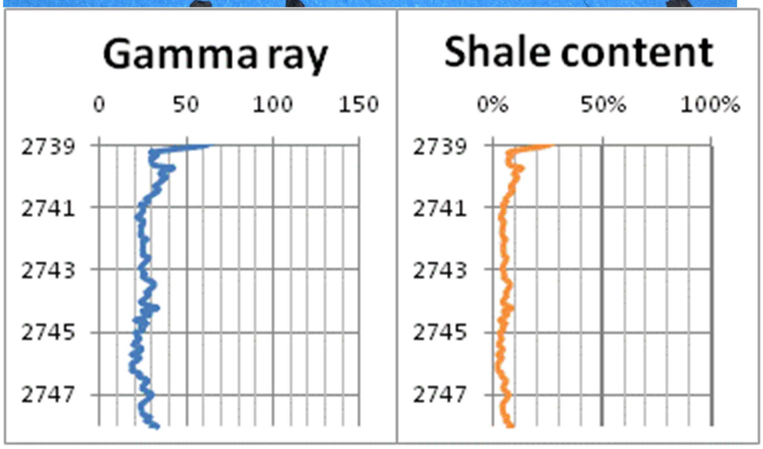

Figure 23 gamma ray log in API and Shale content in volume percent from the interval 2739m-2747m of the PNA GT01 well

The first selected interval of the Delft Sandstone member is a sand deposit of 10 meters in thickness.

This interval consists for 95% out of non-shale content.

Interval 2748- 2757

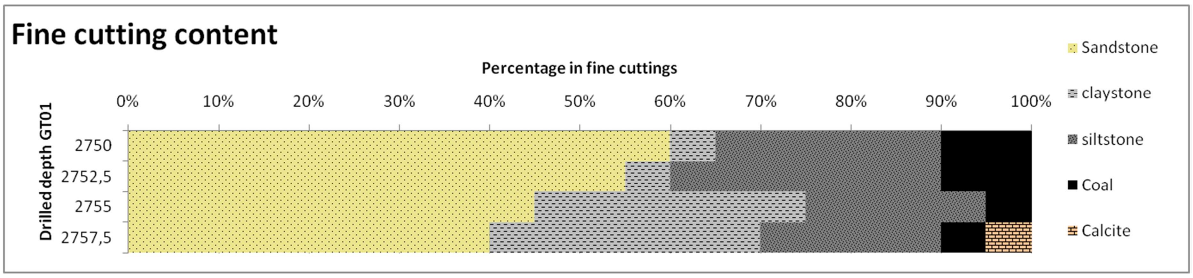

Figure 24GT01 PNA 2752,5 fine fraction (0,064mm-1mm) dried cutting sample.

4. Coal
5. Dark Grey Siltstone
6. Quartz (no cement)

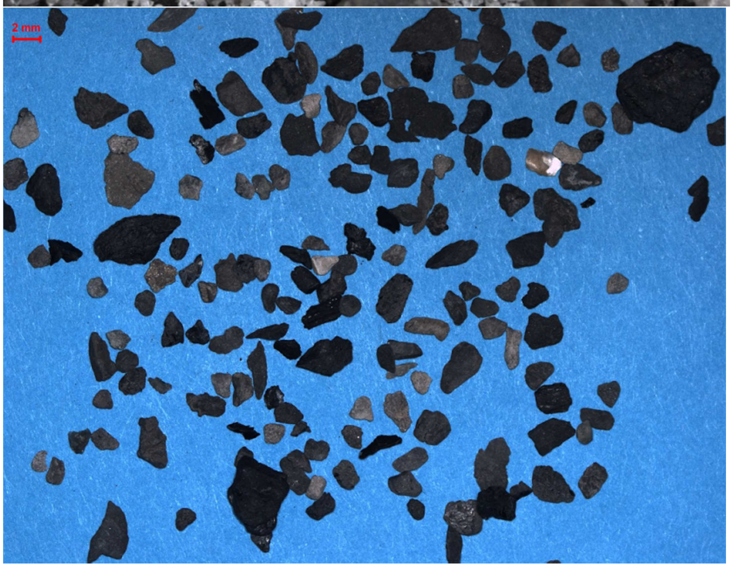

Figure 25GT01 PNA 2750 course fraction (1mm-2mm) dried cutting sample. The scale bar in the top left depicts 2mm.

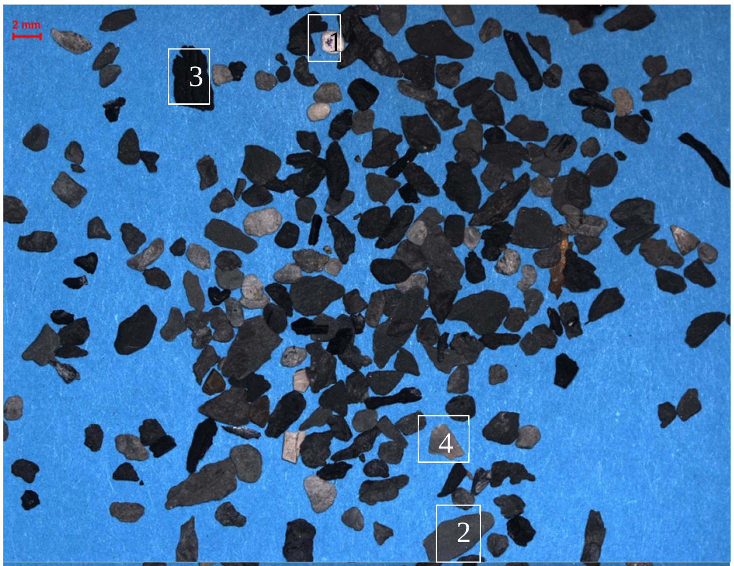

Figure 26 GT01 PNA 2752,5 course fraction (1mm-2mm) dried cutting sample. The scale bar in the top left depicts 2mm.

1. Cemented Quartz
2. Medium grey Claystone
3. Coal
4. Calcite

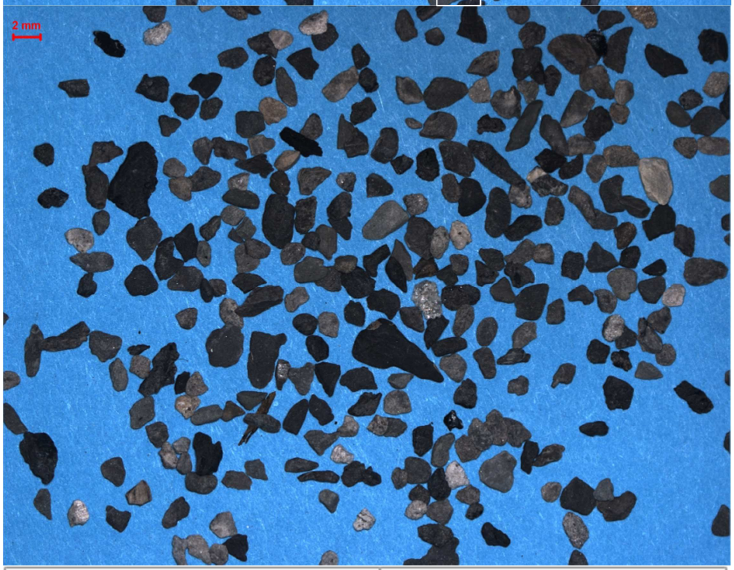

Figure 27 GT01 PNA 2750 course fraction (1mm-2mm) dried cutting sample. The scale bar in the top left depicts 2mm.

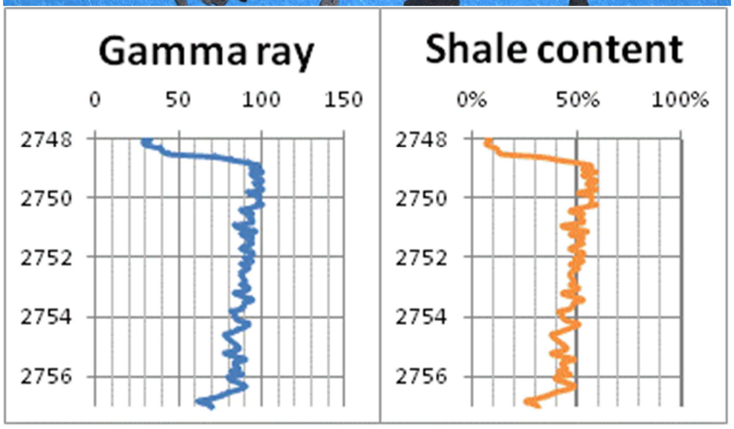

Figure 28 gamma ray log in API and Shale content in volume percent from the interval 2748m-2757m of the PNA GT01 well

The second chosen interval shows a high shale volume percentage of 50% in average. This increases the gamma ray log. It still has a lot of quartz in the fine fractions.

Interval 2757-2763

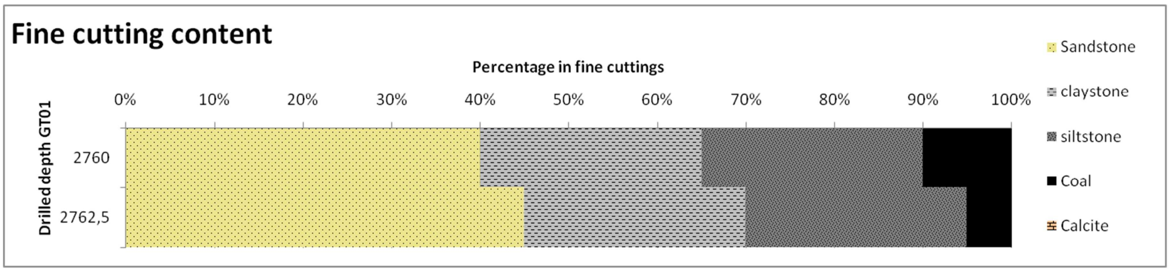

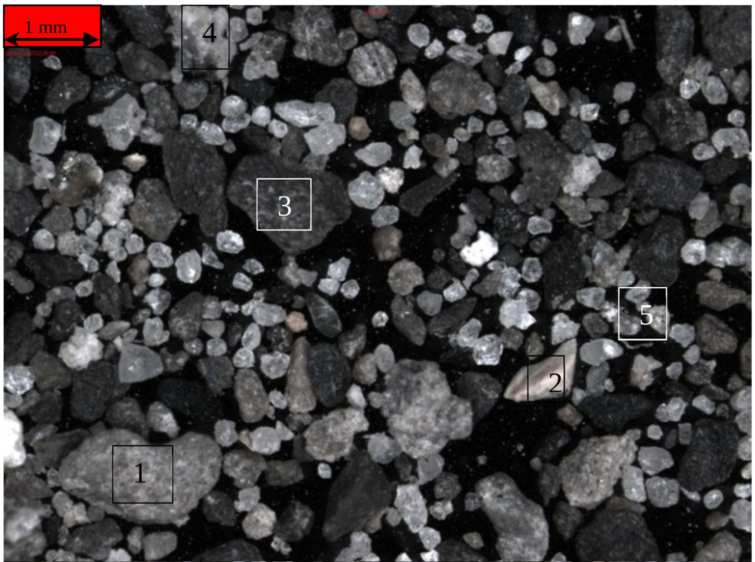

Figure 29 GT01 PNA 2757,5 fine fraction (0,064mm-1mm) dried cutting sample.

1. Medium grey claystone
2. Calcite
3. Dark grey siltstone
4. Cemented Quartz
5. Quartz

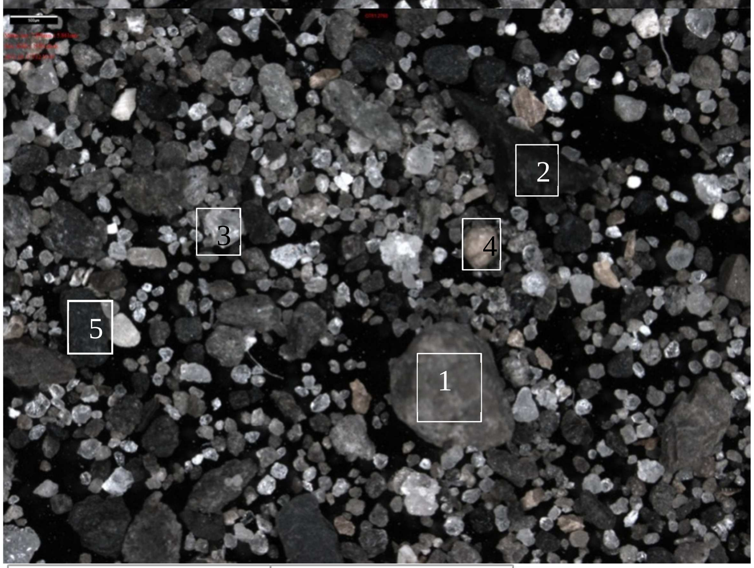

Figure 30 GT01 PNA 2760 fine fraction (0,064mm-1mm) dried cutting sample.

1. Medium grey claystone
2. Coal
3. Quartz
4. Fossil Shell
5. Dark grey siltstone

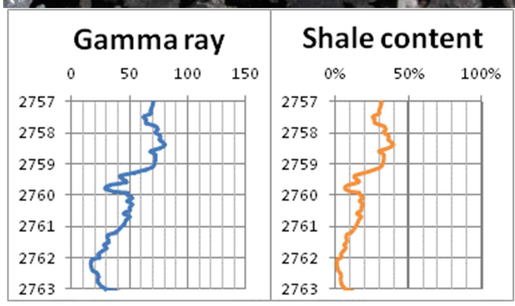

Figure 31 gamma ray log in API and Shale content in volume percent from the interval 2757m-2763m of the PNA GT01 well

This interval shows a decrease in natural radiation. This can be interpreted as a fining upward sequence of a point bar.

Interval 2763-2770

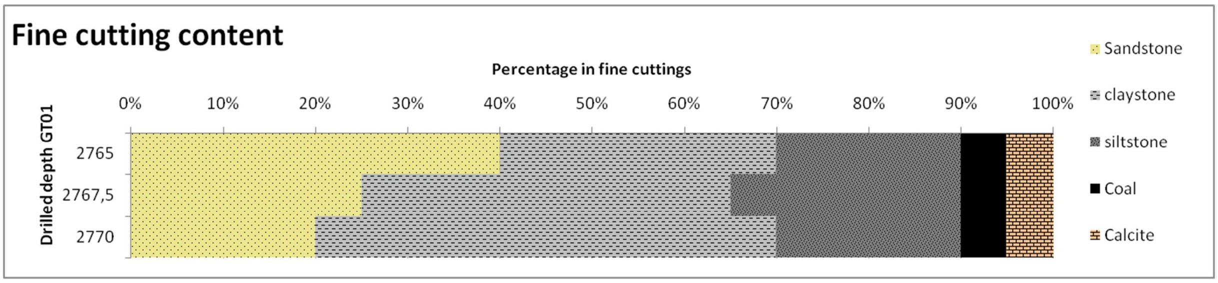

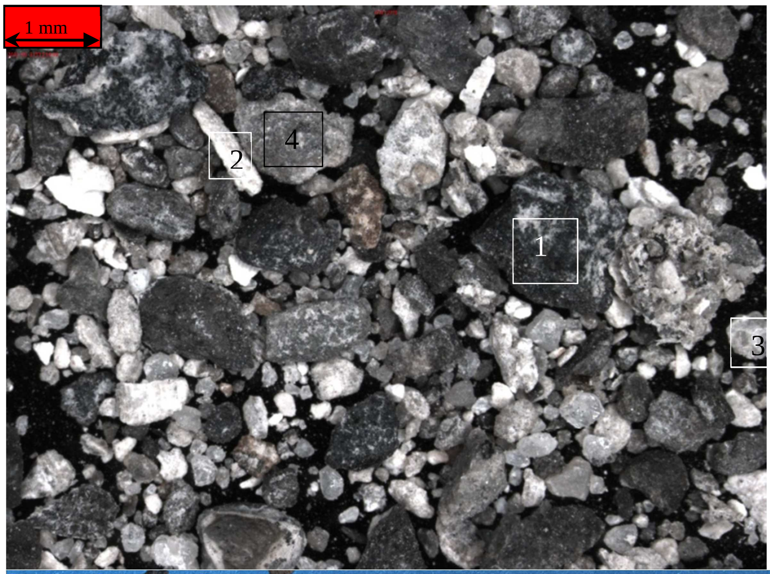

Figure 32 GT01 PNA 2770 fine fraction (0,064mm-1mm) dried cutting sample.

1. Dark grey siltstone
2. Quartz cement
3. Quartz
4. grey claystone

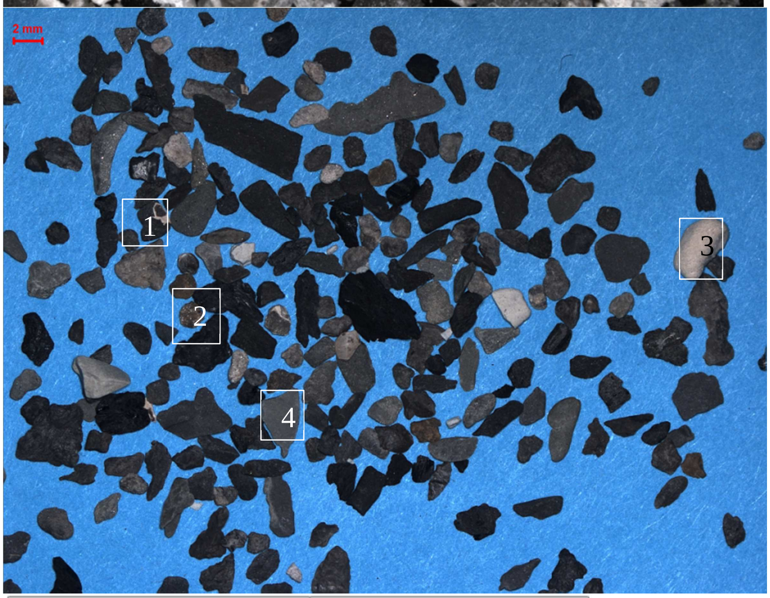

Figure 33 GT01 PNA 2770 course fraction (1mm-2mm) dried cutting sample. The scale bar in the top left depicts 2mm.

1. Coal with fossil
2. Pyrite
3. Cemented Quartz
4. Medium grey Claystone

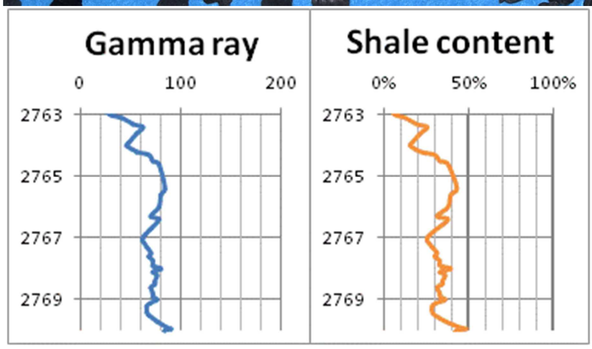

Figure 34 gamma ray log in API and Shale content in volume percent from the interval 2763m-2770 of the PNA GT01 well

This interval shows a relative high shale content and high natural radiation in comparison to other intervals. There are many small clay particles in the rock. The high peak at 2770 meters may be a flood plain.

Interval 2770-2778

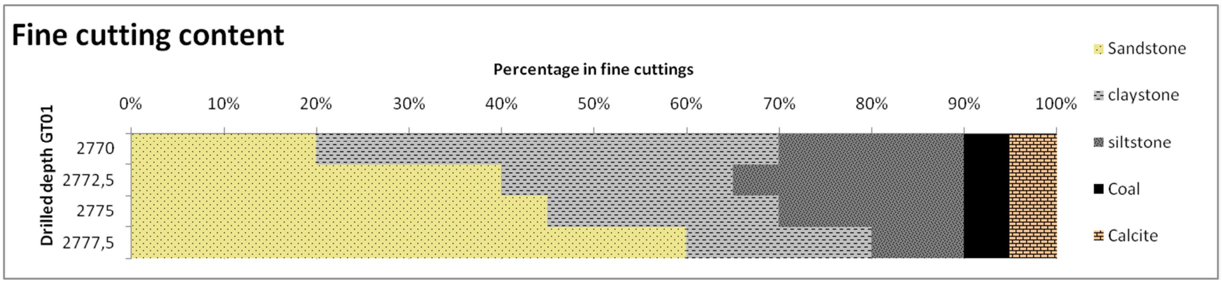

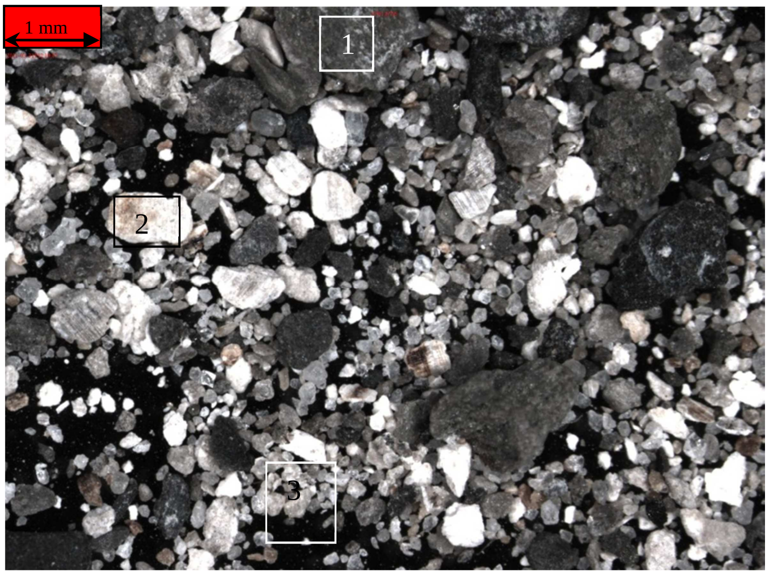

Figure 35 GT01 PNA 2772,5 fine fraction(0,064mm-1mm) dried cutting sample.

1. Medium grey siltstone
2. Light grey claystone
3. Fine upper quartz

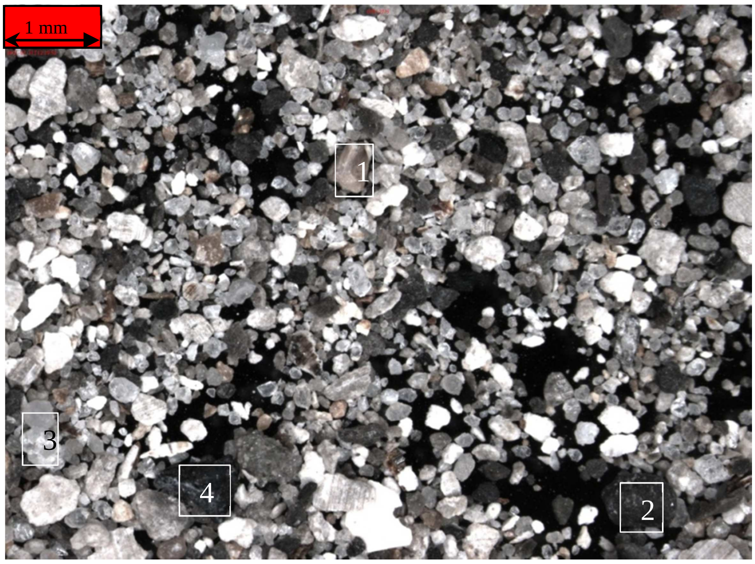

Figure 36 GT01 PNA 2775 fine fraction (0,064mm-1mm) dried cutting sample.

1. Calcite
2. Grey siltstone
3. Quartz
4. Coal

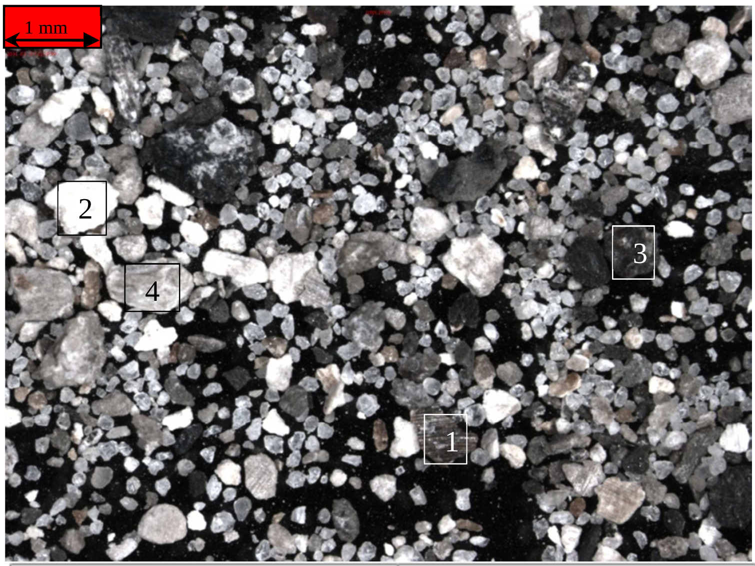

Figure 37 GT01 PNA 2777,5 fine fraction(0,064mm-1mm) dried cutting sample.

1. Layered Calcite
2. Cemented Quartz
3. Dark grey siltstone
4. Light grey claystone

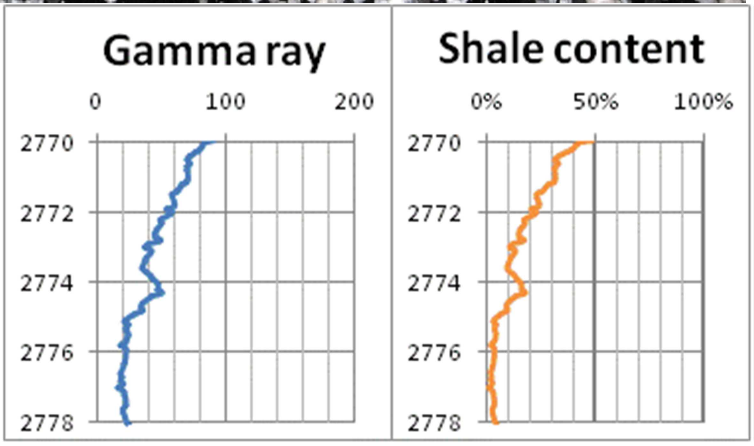

Figure 38 gamma ray log in API and Shale content in volume percent from the interval 2770m-2778m of the PNA GT01 well

This interval shows the gradual decrease in natural radiation and so in shale content. This can be interpreted as a fining upward sequence found in point bars in fluvial deposits.
A Quartz grain size increase is visible. Though this needs further tests. (Recommendations)

Interval 2778-2788

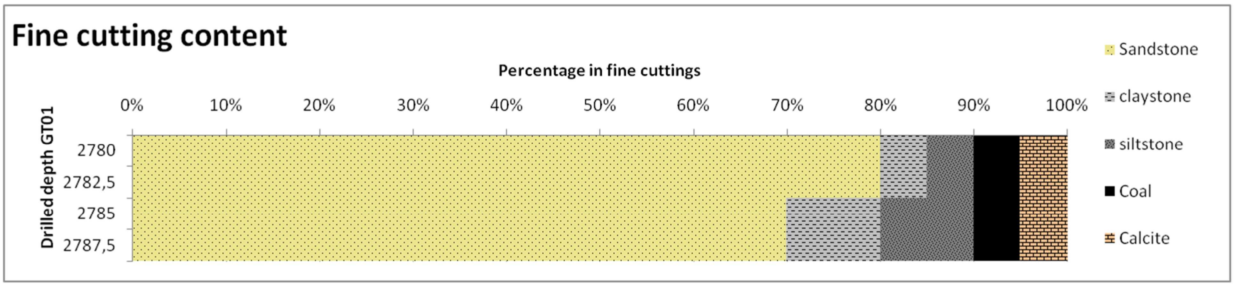

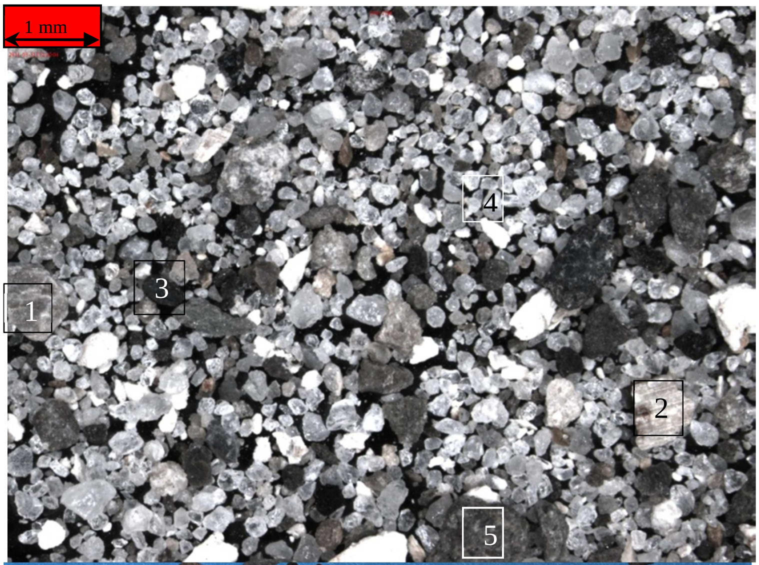

Figure 39 GT01 PNA 2785 fine fraction(0,064mm-1mm) dried cutting sample.

1. Grey claystone
2. Laminated calcite
3. Coal
4. Quartz (no cement)
5. Grey siltstone

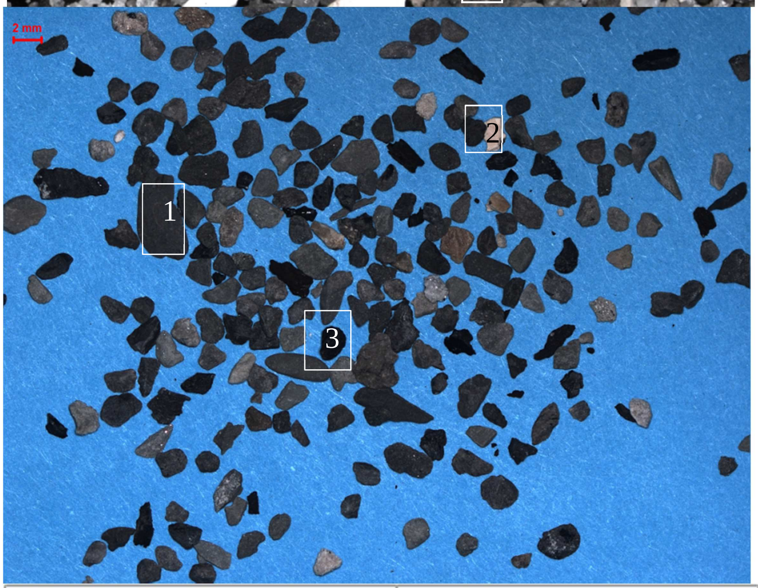

Figure 40 GT01 PNA 2780 course fraction (1mm-2mm) dried cutting sample. The scale bar in the top left depicts 2mm.

1. Dark grey claystone
2. Laminated calcite
3. coal

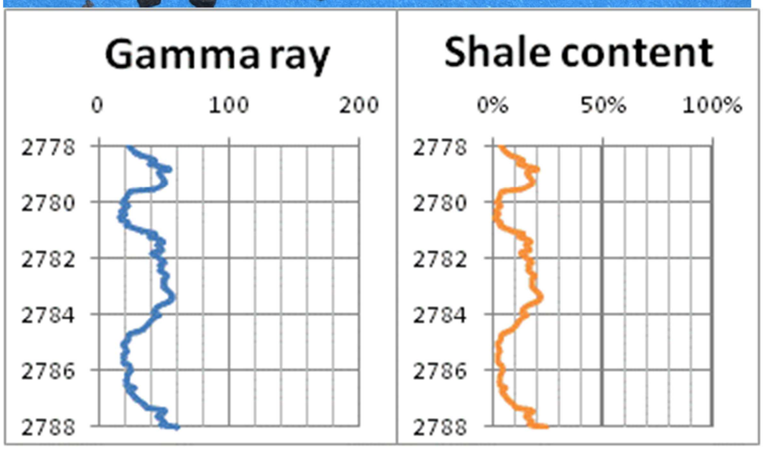

Figure 41 gamma ray log in API and Shale content in volume percent from the interval 2778m-2788m of the PNA GT01 well

Two low natural radiation layers can be seen, and two slightly higher radiating layers in sequence. These can be two flow channels.

Interval 2788-2796

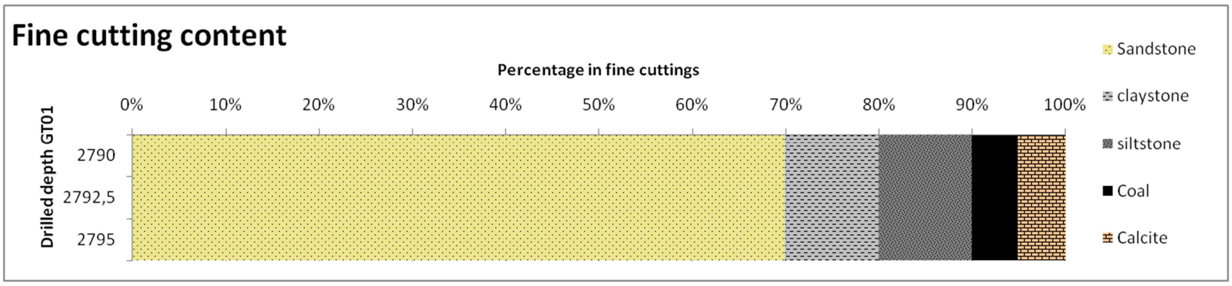

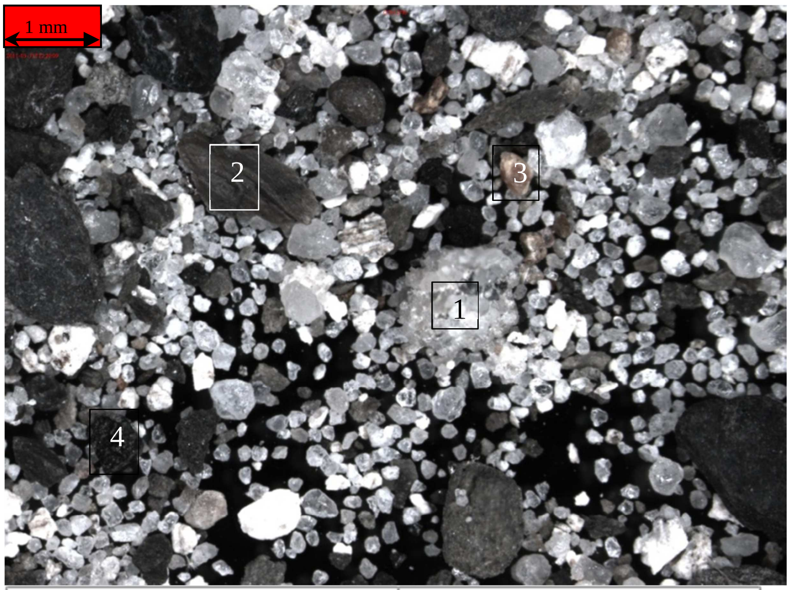

Figure 42 GT01 PNA 2795 fine fraction(0,064mm-1mm) dried cutting sample.

1. Cemented Quartz
2. Grey siltstone
3. Orange brown calcite
4. Coal

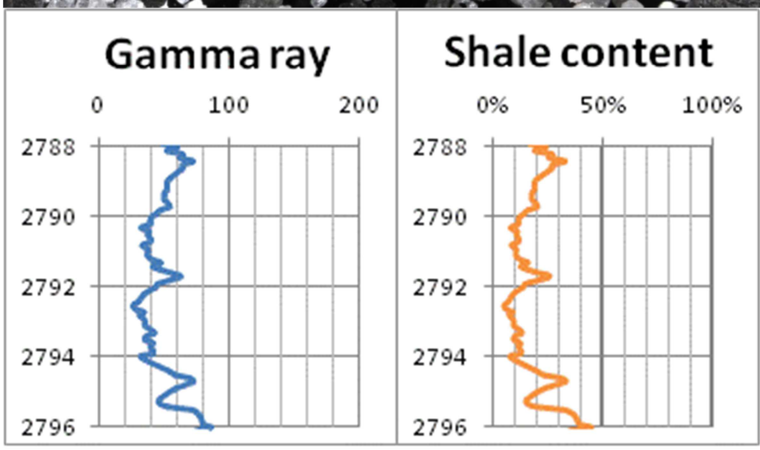

Figure 43 gamma ray log in API and Shale content in volume percent from the interval 2788m-2796m of the PNA GT01 well

The interval shows both high quartz content and shale content. The quartz grains are cemented in this section.

Interval 2796-2811

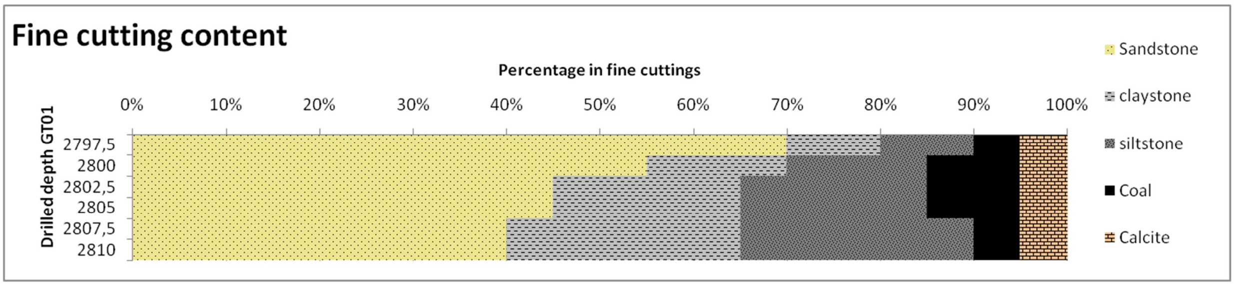

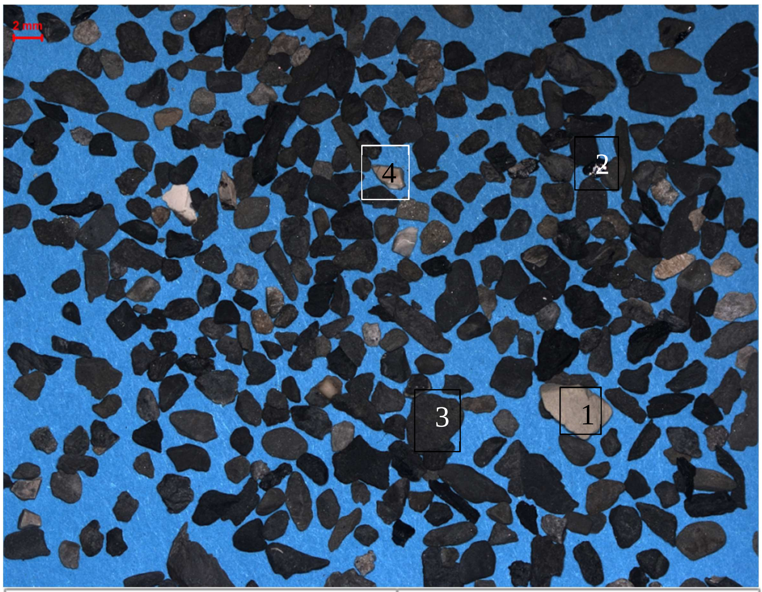

Figure 44 GT01 PNA 2800 course fraction(1mm-2mm) dried cutting sample. The scale bar in the top left depicts 2mm.

1. Light siltstone
2. Coal
3. Dark grey claystone
4. Calcite

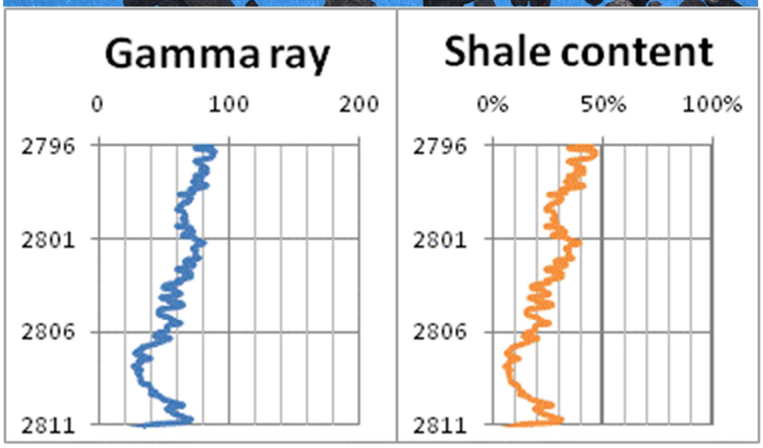

Figure 45 gamma ray log in API and Shale content in volume percent from the interval 2796m-2811m of the PNA GT01 well

This interval shows again a gradual decrease in shale content. This can be interpreted as a fining upward sequence in a point bar.

Interval 2811-2814

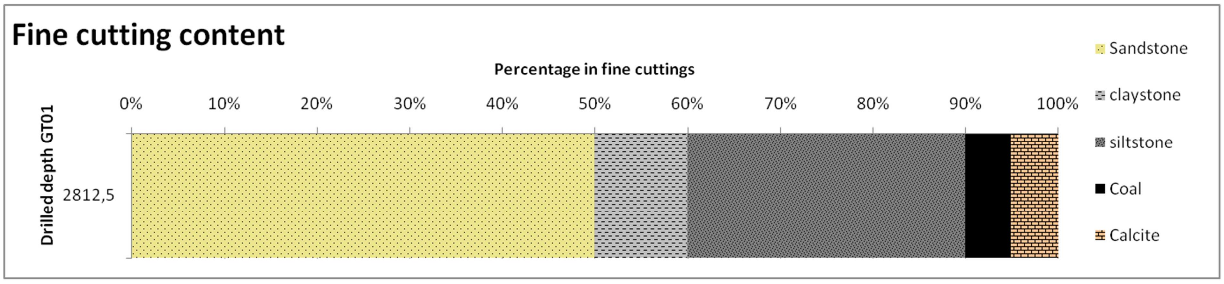

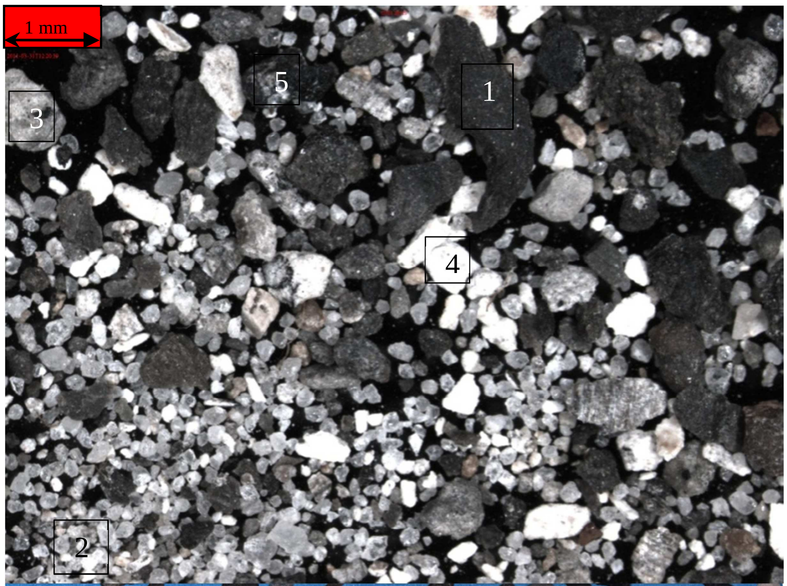

Figure 46 GT01 PNA 2812.5 fine fraction(0,064mm-1mm) dried cutting sample.

1. Dark grey siltstone
2. Quartz with cement
3. Light grey claystone
4. Quartz cement
5. Coal

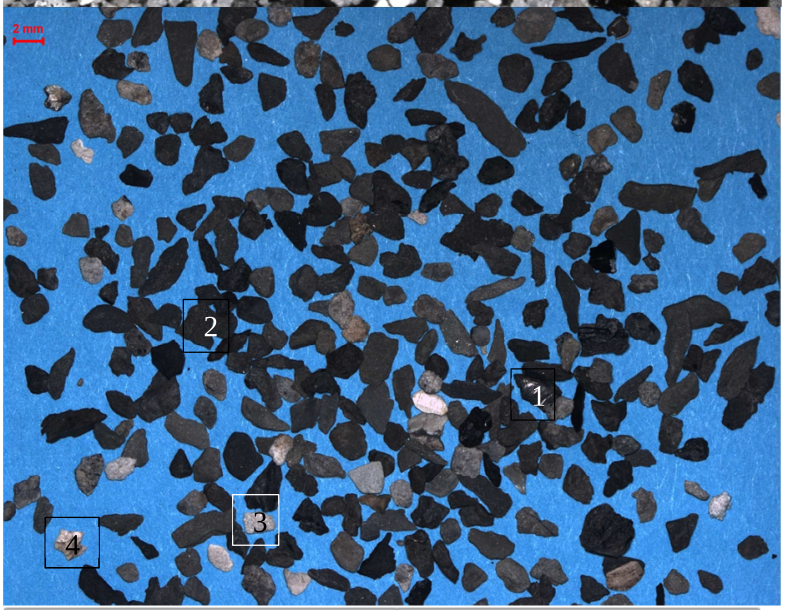

Figure 47 GT01 PNA 2812,5 course fraction(1mm-2mm) dried cutting sample. The scale bar in the top left depicts 2mm.

1. Coal
2. Dark grey claystone
3. Cemented Quartz
4. Calcite

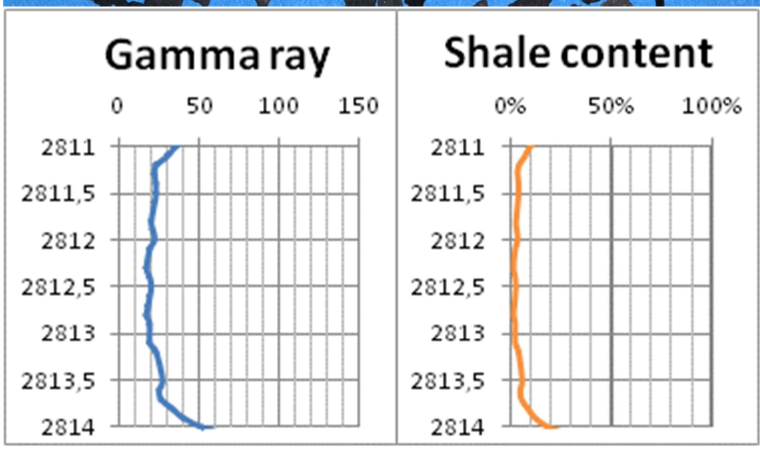

Figure 48 gamma ray log in API and Shale content in volume percent from the interval 2811m-2814m of the PNA GT01 well

A low shale content section. The cuttings show cemented quartz. The quantity of the dried cuttings was low and probably a lot of the silt fraction is flushed in this interval.

Interval 2814-2818

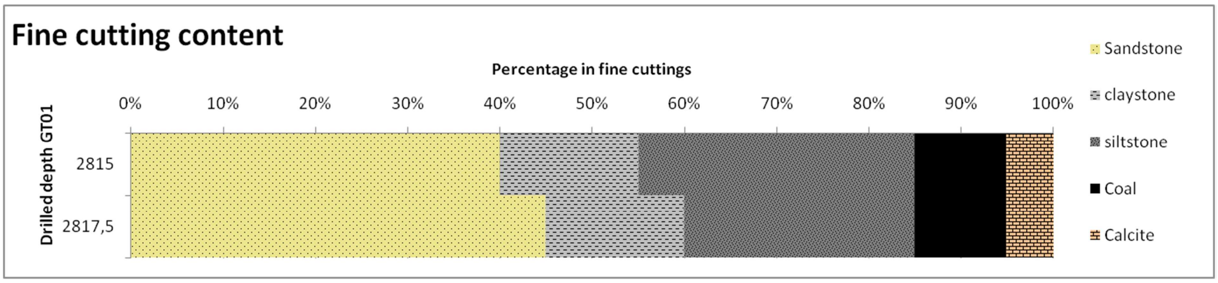

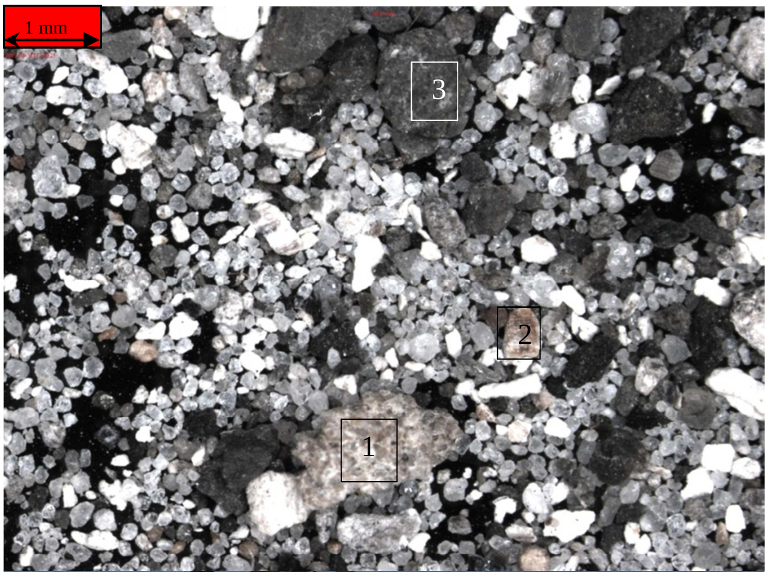

Figure 49 GT01 PNA 2815 fine fraction(0,064mm-1mm) dried cutting sample.

1. Cemented quartz
2. Layered calcite
3. Dark grey siltstone

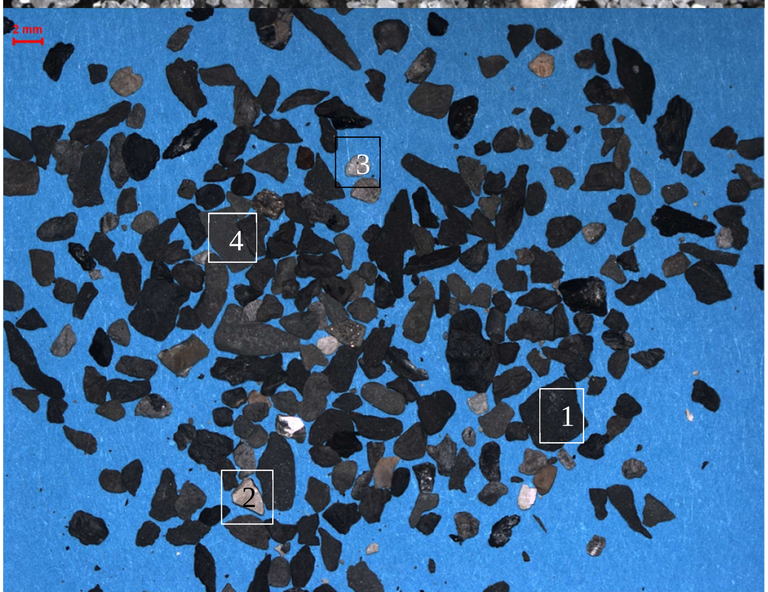

Figure 50 GT01 PNA 2815 course fraction(1mm-2mm) dried cutting sample. The scale bar in the top left depicts 2mm.

1. Coal
2. Calcite
3. Cemented quartz
4. Dark grey claystone

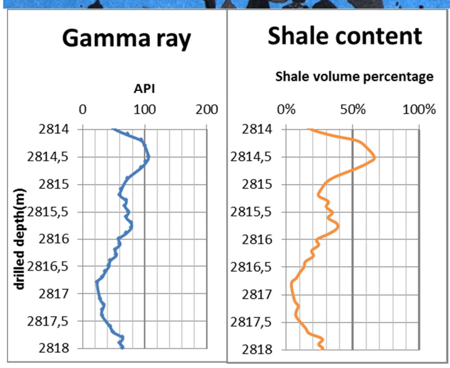

Figure 51 gamma ray log in API and Shale content in volume percent from the interval 2814m-2818m of the PNA GT01 well

At 2814,5 a peak in gamma radiation occurs. This can be interpreted as a clay layer. At 2817,5 low gamma ray and dominance in quartz show a new sand layer.

Interval 2818-2825

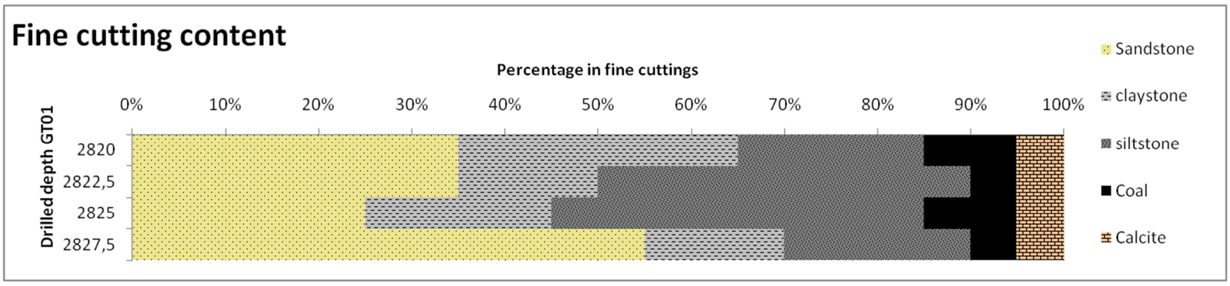

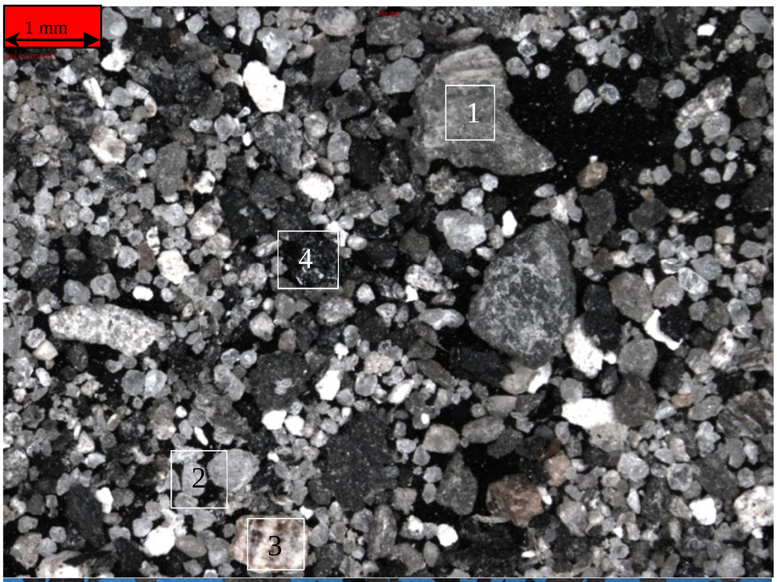

Figure 52 GT01 PNA 2825 fine fraction(0,064mm-1mm) dried cutting sample.

1. Medium grey Claystone
2. Quartz with cement
3. Calcite
4. Coal

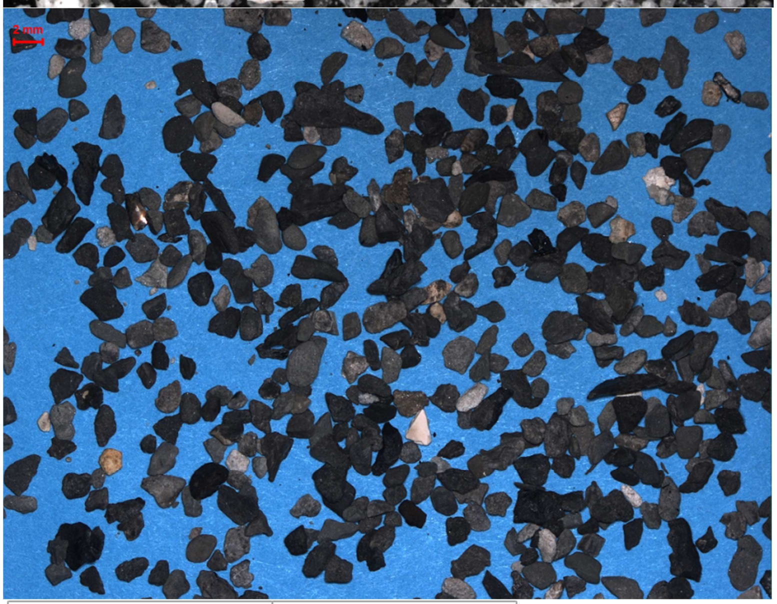

Figure 53 GT01 PNA 2822,5 course fraction(1mm-2mm) dried cutting sample. The scale bar in the top left depicts 2mm.

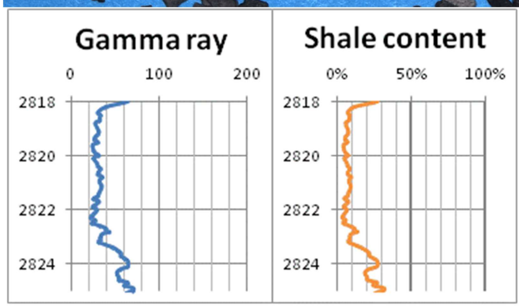

Figure 54 gamma ray log in API and Shale content in volume percent from the interval 2818m-2825m of the PNA GT01 well

The bottom of the Delft Sandstone Member can be determined at the end of this sandstone layer at 2825m drilled depth.

Interval 2825- Alblasserdam

The Alblasserdam is a silt deposit. In the Delft Sandstone one or two fossils could be found per interval. In the cutting sample of 2822,5 eight fossils were found.

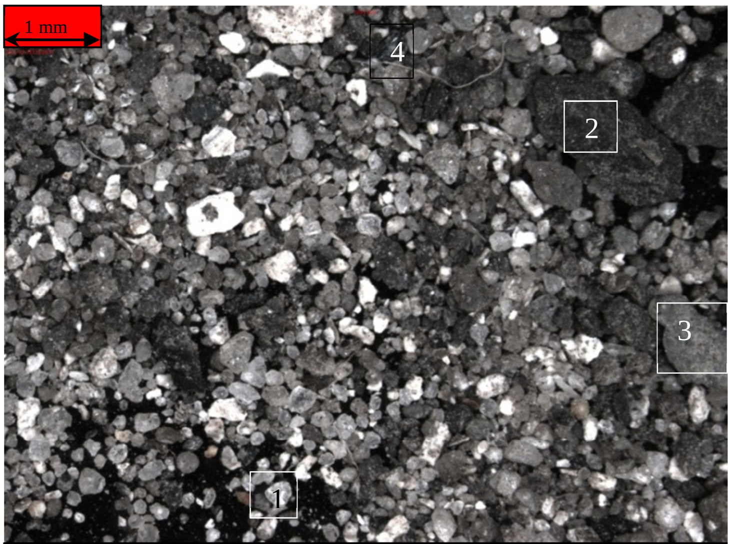

Figure 55 GT01 PNA 2830 fine fraction(0,064mm-1mm) dried cutting sample.

1. Some Quartz
2. Dark grey claystone
3. Light grey siltstone
4. Coal

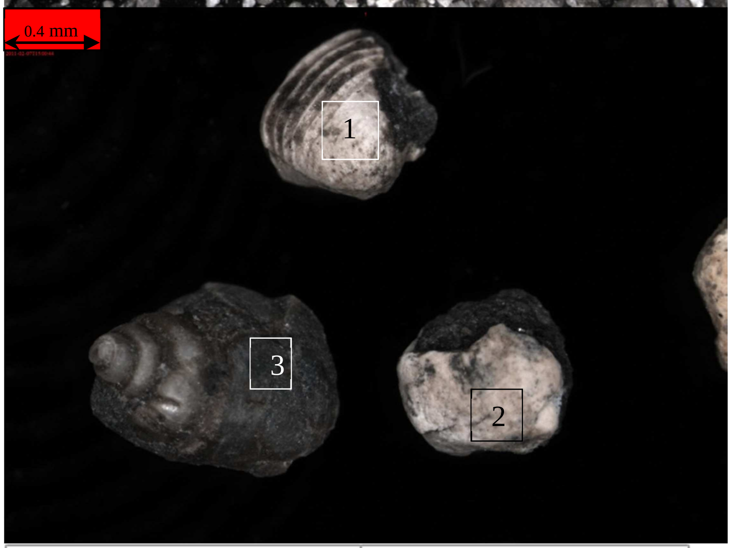

Figure 56 GT01 PNA 2822,5 close-up of shells found in the course cutting samples.

The top of the Alblasserdam member is the first time in this analysis a turbinate shell like number three can be seen in the cuttings. This could aid in the determination of the top for future reservoirs.

1. Patelliform Shell
2. Petelliform Shell
3. Turbinate shell

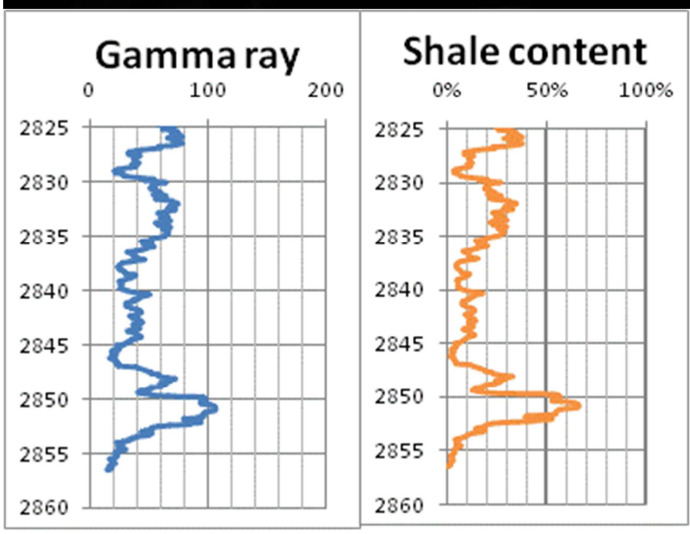

Figure 57 gamma ray log in API and Shale content in volume percent from the interval 2825m-2858m of the PNA GT01 well

The Alblasserdam shows light siltstones and fossils. Low shale content layers can be seen in the gamma ray.

Hydrocarbon content in wet cutting samples

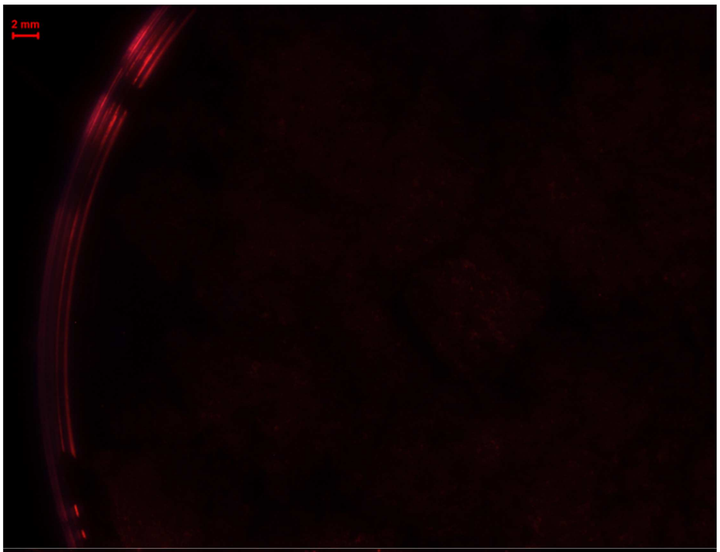

Figure 58 GT01 PNA 2702,5 wet cutting sample under UV light. The scale bar in the top left depicts 2mm.

As an example the wet cuttings of interval 2702,5 are depicted. Here no fluorescent reaction is to be seen. No hydrocarbon is present in the reservoir at this clay layer in the Rodenrijs Claystone.

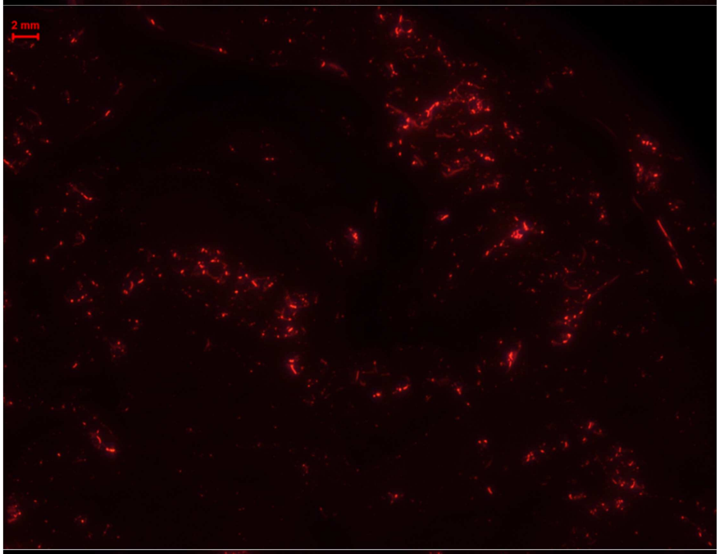

Figure 59 GT01 PNA 2745 wet cutting sample under UV light. The scale bar in the top left depicts 2mm.

This is the first sand interval 10 meters in thickness at the top of the Delft Sandstone group. Under UV lighting fluorescent light is showing due to hydrocarbon presence.

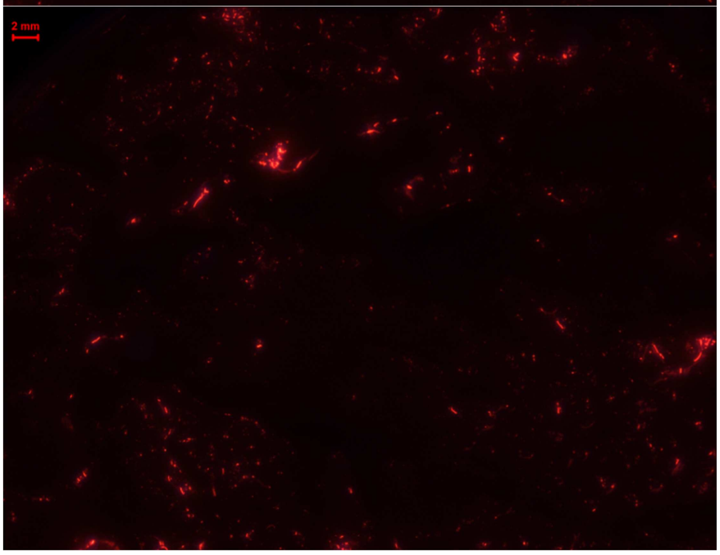

Figure 60 GT01 PNA 2762,5 wet cutting sample under UV light. The scale bar in the top left depicts 2mm.

This is the second interval with a low shale-volume percentage. Here too hydrocarbons react fluorescent to the UV light.

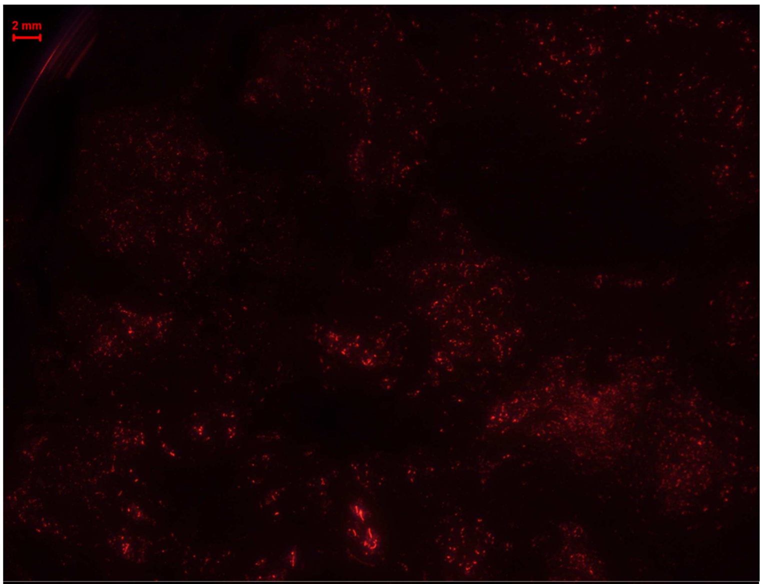

Figure 61 GT01 PNA 2775 wet cutting sample under UV light. The scale bar in the top left depicts 2mm.

Fluorescence shows hydrocarbon presence in this interval.

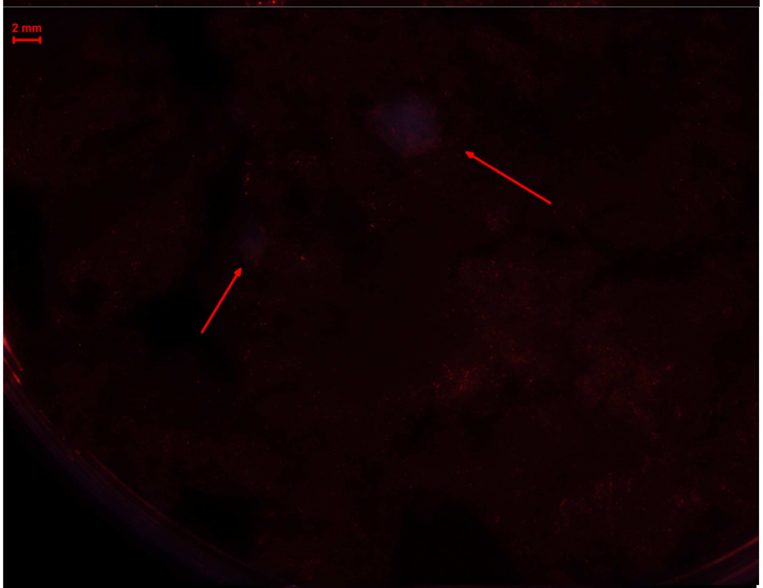

Figure 62 GT01 PNA 2785 wet cutting sample under UV light. The scale bar in the top left depicts 2mm.

Due to white substances (pointers indicate these) in the wet cutting sample the image could not show the hydrocarbons fluoresce. They can be seen in the red square. This interval too shows hydrocarbon content.

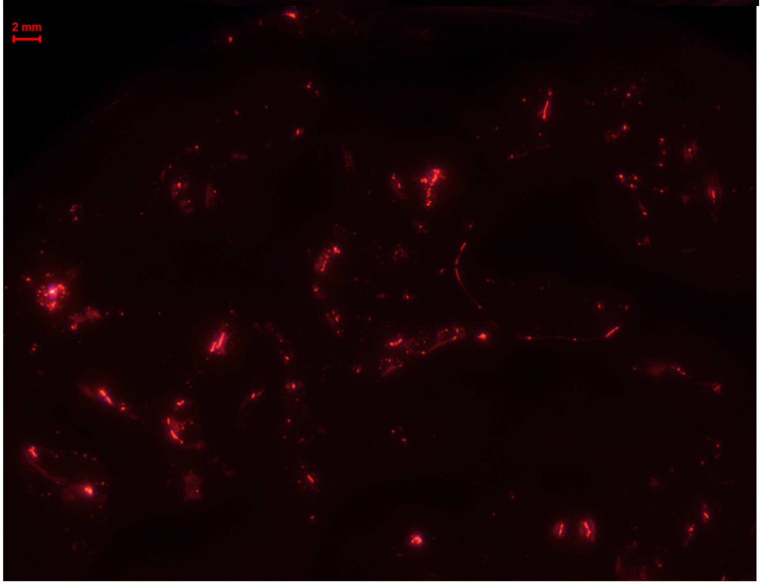

Figure 63 GT01 PNA 2812,5 wet cutting sample under UV light. The scale bar in the top left depicts 2mm.

The hydrocarbon presence is clearly visible in this wet cutting sample.

This is the interval with the most visible result tested.

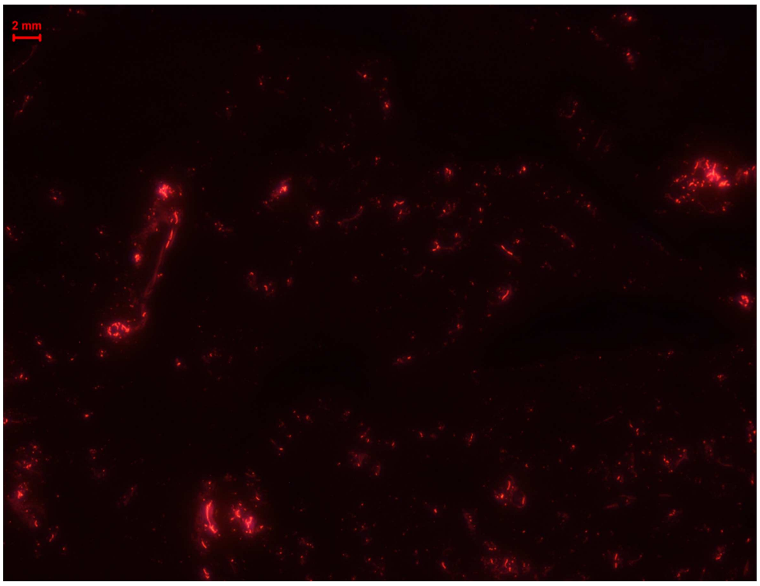

Figure 64 GT01 PNA 2820 wet cutting sample under UV light. The scale bar in the top left depicts 2mm.

The bottom sand structure of the Delft Sandstone Member shows hydrocarbon presence.

Hydrocarbon fluorescence in dried cutting samples

Hydrocarbon content in dried cutting samples is less clearly visible. The brightest marks to be seen in the images taken of these cuttings are dust particles. Even though the hydrocarbons still show under UV light, the results are less obvious to the eye.

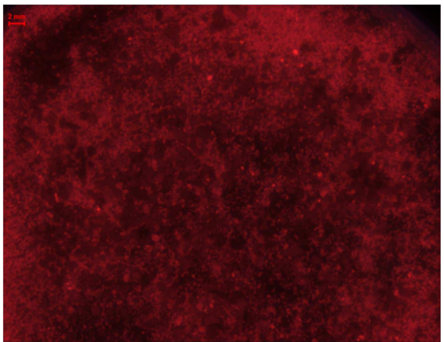

Figure 65 GT01 PNA 2745 dried cutting sample under UV light. The scale bar in the top left depicts 2mm.

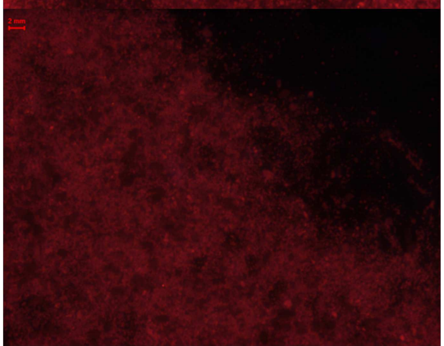

Figure 66 GT01 PNA 2785 dried cutting sample under UV light. The scale bar in the top left depicts 2mm.

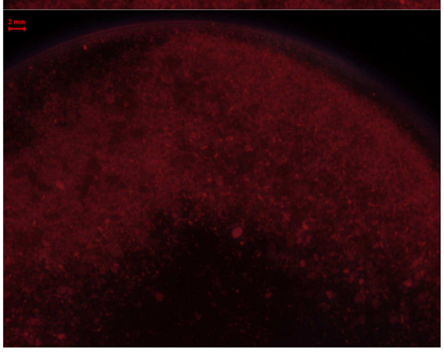

Figure 67 GT01 PNA 2820 dried cutting sample under UV light. The scale bar in the top left depicts 2mm.

Content of cutting samples – fine fraction

The fine fraction cutting analysis was conducted using the stereomicroscope. The rounding is of the quartz grains.

depth	main fraction	rounding	content					
2735	Grey silt	subangular	grey silt	lignite	layered calcite	darkgrey clay	cemented quartz	
2737,5	Grey silt	subangular	grey silt	cemented quartz	quartz	layered calcite	Rodenrijs claystone	
2740	Grey silt	subrounded	grey silt	quartz	lignite	layered calcite	chalcedone	
2742,5	Quartz	spherical	quartz	layered calcite	lignite	grey silt		
2745	Quartz	spherical	quartz	lignite	grey silt	cemented quartz		
2747,5	Quartz	subangular	quartz	lignite	pyrite	cemented quartz		
2750	Quartz	subangular	quartz	lignite	grey silt			
2752,5	Quartz	subrounded	quartz	grey silt	cemented quartz	pyrite		
2755	Quartz/Grey silt	subrounded	quartz	grey silt	cemented quartz			
2757,5	Quartz/Grey silt 60/40	subangular	quartz	grey silt	calcite	lignite	cemented quartz	
2760	Quartz/Grey silt 60/40	subangular	quartz	grey silt	lignite	calcite		
2762,5	Grey silt/Quartz 60/40	subrounded	grey silt	quartz	pyrite	lignite	cemented quartz	calcite
2765	Quartz/Grey silt	angular	grey silt	quartz	calcite	lignite	pyrite	
2767,5	Quartz	subangular	quartz	grey silt	calcite	lignite	pyrite	
2770	Cemented Quartz	angular	cemented qua	grey silt	calcite	pyrite		
2772,5	Grey Silt	subangular	grey silt	quartz	calcite	lignite		
2775	Grey Silt	subangular	grey silt	quartz	calcite	cemented quartz		
2777,5	Quartz	subrounded	quartz	calcite	grey silt			
2780	Quartz	angular	quartz	coal	cemented quartz	calcite		
2782,5	Quartz	subangular	quartz	calcite	grey silt			
2785	Quartz	angular	quartz	calcite	silt			
2787,5	Quartz	subangular	quartz	grey silt	calcite			
2790	Cemented Quartz	subrounded	cemented qua	grey silt	calcite	coal		
2792,5	Quartz	subangular	quartz	cemented quartz	calcite	grey silt	coal	
2795	Quartz	subangular	quartz	cemented quartz	grey silt	coal	calcite	pyrite on quartz
2797,5	Cemented Quartz	subrounded	quartz	cemented quartz	grey silt	calcite		
2800	Cemented Quartz	subangular	quartz	grey silt	cemented quartz	calcite		
2802,5	Cemented Quartz	very angular	cemented qua	grey silt	quartz	pyrite	coal	calcite
2805	Cemented Quartz	subangular	cemented qua	quartz	grey silt	calcite		
2807,5	Cemented Quartz	subangular	quartz	cemented quartz	grey silt	coal	calcite	
2810	Quartz	subrounded	quartz	cemented quartz	grey silt	calcite		
2812,5	Grey silt	angular	grey silt	quartz	calcite	cemented quartz	quartz cement	
2815	Quartz	angular	quartz	quartz cement	cemented quartz	grey silt	calcite	
2817,5	Quartz	angular	quartz	cemented quartz	grey silt	calcite		
2820	Quartz	subrounded	quartz	cemented quartz	calcite	grey silt	coal	
2822,5	Quartz	subrounded	quartz	cemented quartz	calcite	coal	grey silt	Fossils gastropods
2825	Cemented Quartz	subangular	quartz	coal	grey silt	calcite	cemented quartz	
2827,5	Cemented Quartz	subangular	quartz	quartz cement	calcite	grey silt	coal	

Figure 68 Results of the visual analysis of the fine fraction using the stereo microscope. The rounding quartz grains is noted.

Content of cutting samples – course fraction

The course fraction cutting analysis showed in almost all samples the same dominant fraction. The fine fraction and the gamma ray log do support this finding. Cuttings in the coarse fraction show a part of the content but it is better to study the fine fraction first.

depth	dominant fraction	rounding	content				
2735	grey silt	subangular	grey silt	quartz	laminated calcite	cemented quartz	
2737,5	grey silt	angular	grey silt	cemented quartz	lignite	laminated calcite	
2740	grey silt	subrounded	grey silt	lignite	cemented quartz		
2742,5	grey silt	angular	grey silt	cemented quartz	laminated calcite	lignite	
2745	grey silt	subangular	grey silt	laminated calcite	lignite		
2747,5	grey silt	subangular	grey silt	cemented quartz	lignite		
2750	grey silt	angular	grey silt	lignite	cemented quartz		
2752,5	grey silt	angular	grey silt	lignite	cemented quartz		
2755	grey silt	subrounded	grey silt	cemented quartz	laminated calcite	lignite	
2757,5	grey silt	subangular	grey silt	calcite	lignite		
2760	grey silt	subangular	grey silt	lignite	laminated calcite		
2762,5	grey silt	angular	grey silt	laminated calcite	lignite	cemented quartz	
2765	grey silt	subangular	grey silt	cemented quartz	calc	lignite	
2767,5	shale?	rounded	grey silt	lignite	calc	cemented quartz	
2770	grey silt	subangular	grey silt	lignite	calcite		
2772,5	grey silt	well rounded	grey silt	calcite	lignite	cemented quartz	
2775	Error	subangular	grey silt	quartz	calcite	cemented quartz	
2777,5	grey silt	angular	grey silt	lignite	cemented quartz		
2780	grey silt	angular	grey silt	lignite	coal	cemented quartz	
2782,5	grey silt	subangular	grey silt	lignite	calcite	quartz	
2785	grey silt	angular	grey silt	light grey silt	calcite	cemented quartz	coal
2787,5	grey silt	subrounded	grey silt	cemented quartz			
2790	grey silt	subrounded	grey silt	cemented quartz			
2792,5	grey silt	subangular	grey silt	coal	calcite	cemented quartz	
2795	grey silt	subangular	grey silt	cemented quartz	coal	calcite	
2797,5	grey silt	subangular	grey silt	coal	cemented quartz		
2800	grey silt	subrounded	grey silt	coal			
2802,5	grey silt	subangular	grey silt	calcite	cemented quartz		
2805	grey silt	subangular	grey silt	quartz	calcite	coal	
2807,5	grey silt	subangular	grey silt	coal	quartz	cemented quartz	
2810	grey silt	subrounded	grey silt	calcite	coal		
2812,5	grey silt	angular	grey silt	cemented quartz	lignite		
2815	grey silt	angular	grey silt	calcite	cemented quartz	lignite	
2817,5	grey silt	angular	grey silt	cemented quartz	calc	coal	lignite
2820	grey silt	subangular	grey silt	quartz	cemented quartz	coal	
2822,5	grey silt	rounded	grey silt	grey silt	lignite	coal	cemented quartz
2825	Coal	very angular	coal	grey silt	lignite	cemented calcite	
2827,5	grey silt	angular	grey silt	antracite	cemented quartz	lignite	calcite

Figure 69 Results of the visual analysis of the course fraction using the stereo microscope. The rounding is of the quartz grains.

Data from the XRF analysis

```
*****************************************************************************
* TU-Delft*Faculty 3mE  * Section Structure & Change        * R.W.A. Hendrikx *
* Mekelweg 2             * Tel. 015-2782255                   *                 *
* 2628 CD Delft          * Fax  015-2786730                   *                 *
***************Semi-Quantitative XRF analysis *******************************
C:\UQ5\USER\TUD_TA\Jobs\JOB.535    2010-12-20
Delft SST1 Langeveld 20dec10

Spectrometer's configuration:  PW2400 Rh 60kV       Method   : UniQuant
C:\UQ5\USER\TUD_TA\Appl\AnySample.kap 2010-11-10
Calculated as :  Oxides        Matrix (Shape & ImpFc) :  2|SiO2
X-ray path     =  Vacuum       Film type      = No supporting film
Case number    =  0  All known
Eff.Diam.      = 23.0 mm       Eff.Area       = 415.3 mm2
KnownConc      =  0     %
Rest           =  0     %                     Viewed Mass    = 2000.000 mg
Dil/Sample     =  0                           Sample Height = 1.00 mm
           <   means that the concentration is <  50 mg/kg
           <2e  means wt% < 2 StdErr. A + or & means: Part of 100% sum
 Z         m/m%   StdErr   Z          m/m%   StdErr   Z          m/m%   StdErr
=========================  =========================  =========================
SumBe..F   0.133   0.029   29+CuO     <               52 TeO2    <
11+Na2O    0.799   0.088   30+ZnO     0.0114  0.0009  53 I       <
12+MgO     0.519   0.057   31+Ga2O3   <               55 Cs2O    <2e     0.0051
13+Al2O3  14.46    0.23    32 GeO2    <               56+BaO     0.0351  0.0080
14+SiO2   72.47    0.50    33 As2O3   <               SumLa..Lu  0.007   0.048
15+P2O5    0.0524  0.0021  34 SeO2    <               72 HfO2    <
15 P                       35+Br      <               73 Ta2O5   <
16 SO3                     37+Rb2O    0.0076  0.0006  74 WO3     <
16+S       0.233   0.012   38+SrO     0.0142  0.0016  75 Re2O7   <
17+Cl      1.74    0.15    39+Y2O3    <               76 OsO4    <
18 Ar      <               40+ZrO2    0.0393  0.0020  77 IrO2    <
19+K2O     3.78    0.21    41 Nb2O5   <               78 PtO2    <
20+CaO     2.58    0.18    42+MoO3    0.0055  0.0014  79 Au      <
21 Sc2O3   <               44+RuO2    <               80 HgO     <
22+TiO2    0.731   0.081   45+Rh2O3   <               81 Tl2O3   <
23+V2O5    0.0162  0.0014  46+PdO     <               82 PbO     <
24+Cr2O3   0.0223  0.0025  47 Ag2O    <               83 Bi2O3   <
25+MnO     0.0219  0.0014  48 CdO     <               90 ThO2    <
26+Fe2O3   2.31    0.17    49 In2O3   <               92 U3O8    <
27 Co3O4   <               50 SnO2    <               94 PuO2
28+NiO     <               51 Sb2O3   <               95 Am2O3

=== Light Elements =====  === Noble Elements =====  ==== Lanthanides ======
SumBe..F   0.133   0.029   44+RuO2    <               57 La2O3   <
 4 BeO                     45+Rh2O3   <               58 CeO2    <
 5 B2O3                    46+PdO     <               59 Pr6O11  <
 6 CO2                     47 Ag2O    <               60 Nd2O3   <
 7 N                       75 Re2O7   <               62 Sm2O3   <
 8 O                       76 OsO4    <               63 Eu2O3   <
 9+F       0.133   0.029   77 IrO2    <               64 Gd2O3   <
                           78 PtO2    <               65 Tb4O7   <
                           79 Au      <               66 Dy2O3   <
                                                      67 Ho2O3   <
                                                      68+Er2O3   <
                                                      69 Tm2O3   <
                                                      70 Yb2O3   <
                                                      71 Lu2O3   <

KnownConc= 0                    REST= 0                   D/S= 0
Sum Conc's before normalisation to 100% :    89.7 %
Total % stripped Oxygen: 48.247
```

Figure 70 Results from the XRF analysis from De Leeuw and Langeveld, 2010